1. Leg 200 Synthesis: A Broadband Seismic Station in Oceanic Crust at the Hawaii-2 Observatory and Coring into the Nuuanu Landslide[1]

Junzo Kasahara[2] and Ralph Stephen[3]

ABSTRACT

Two sites were drilled during Ocean Drilling Program Leg 200: the Hawaii-2 Observatory (H2O) site (Site 1224) and the Nuuanu Landslide site (Site 1223). In Hole 1224D we drilled basaltic basement to 59 meters below seafloor (mbsf) and installed a reentry cone with cemented casing for future installation of a borehole broadband seismometer. During operations at the H2O site, broadband seismometer records obtained from the shallowly buried H2O seismometer were analyzed. In the midocean, the traditional "double-frequency" microseism peak splits into two peaks associated with different kinds of noise sources. Microseism levels in the band ~0.2–0.5 Hz correlated with sea state and wind speed observed from the drillship, indicating that this noise is generated locally at the sea surface. Microseism levels in the band 0.1–0.2 Hz correlate with high sea states impacting distant shorelines. Large quasi-periodic noise generated by whales and drilling-related noise were also identified. Also during Leg 200, a 3.5-kHz source attached to the camera sled on the drill string was lowered to near the seafloor to improve lateral resolution and depth penetration of the echo-sounding records. Acoustic pings were acquired on the ship's hull-mounted echo-sounding system and processed onboard.

Hole 1224F, 20 m away from Hole 1224D, was drilled to 173.5 mbsf. Drilling in Hole 1224F recovered >100 m of ~46-Ma basaltic basement that comprises of three units. Although these three units are geochemically distinct, they are more highly evolved than most mid-ocean-ridge

basalt (i.e., they have experienced a protracted history of cooling and crystal fractionation within the crust). Most basalts are <5% altered to secondary mineral assemblages of Fe oxyhydroxides, celeadonite, saponite, Ca carbonate, trace pyrite, and rare phillipsite and quartz. Ca carbonate formed within 20 m.y. of crustal formation and at low temperatures (4°–11°C). Logging and physical property measurements correlate well with lithology, geochemisty, and alteration of minerals in basalt. Fractures and low-temperature alteration greatly reduce V_P, suggesting a cause of V_P ~ 4.5 km/s in oceanic Layer 2B. Microbiological analyses discovered fungi in calcite veins in abyssal basalts, evidence that eukaryotic life existed in this extreme environment below the seafloor.

The Nuuanu Landslide site, ~260 km northeast of the island of Oahu near the crest of the 500-m-high Hawaiian Arch, was also drilled. We drilled to 41 mbsf and identified eight sandy layers. The layers contain fresh and angular glass fragments typical of Hawaiian shield volcanoes. Degassed glasses are estimated to be subaerially erupted. Seven of the sandy layers are thought to be associated with the Koolau Landslide prior to 1.77 Ma. Of the four thicker sandy layers, it is unclear which are related to the Nuuanu Landslide. Analysis of the Site 1223 cores suggests repeated occurrences of collapsing Hawaiian volcanoes and debris flows to ~260 km distance.

INTRODUCTION

Ocean Drilling Program (ODP) Leg 200 had two distinct objectives:

1. Drill a borehole for long-term seismic observations at the Hawaii-2 Observatory (H2O; Site 1224) (Stephen, Kasahara, Acton, et al., 2003), and
2. Sample the marginal portions of the Nuuanu Landslide (Site 1223) (Fig. F1).

In order to understand the nature of the Earth, it is extremely important to study both spatial and temporal changes. Traditional sea-going expeditions primarily study spatial variations, which because of seafloor spreading can be used as a proxy for processes over geological timescales. On the other hand, submarine cabled observatories enable real-time temporal monitoring of oceanographic, biological, chemical, geological, and geophysical processes. The U.S. Ocean Research Interactive Observatory Network (ORION) project (ORION, 2004), the Japanese Geophysical and Oceanographical TransOcean Cable (GeO-TOC) project (Kasahara et al., 1998), and the Japanese Versatile Eco-monitoring Network by Undersea-cable System (VENUS) project (Kasahara, 2000; Kasahara et al., 2001, 2003) are examples of projects targeted at real-time acquisition. A broad range of seafloor measurements either require, or are improved by, borehole installations (Stephen et al., 2003), and borehole observatories are a natural complement to cabled observatories.

The second objective of Leg 200 was to drill a hole in the Nuuanu Landslide to explore the nature of the gigantic Koolau Landslide. Bathymetric surveys and piston core samples taken east of Oahu show that Koolau Volcano on Oahu experienced a gigantic collapse of the northeast part of the volcano ~2 m.y. ago (Figs. F2, F3). This collapse generated the Nuuanu Landslide, which we found was actually a series of landslides. The turbidite deposits caused by these landslides are found
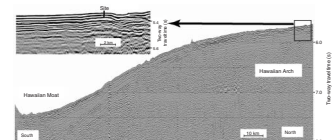
F1. Location map, p. 18.
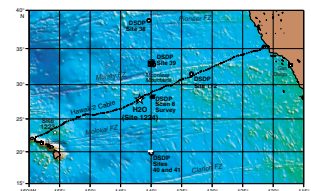
F2. Nuuanu Landslide, p. 19.
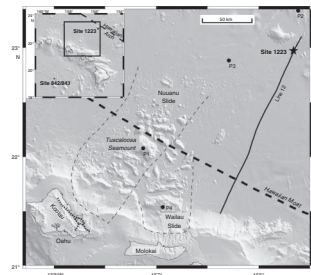
F3. Seismic reflection record along Line 12, p. 20.

200 km away from Oahu, and it was estimated that turbidites could be found even farther away. It was planned to study the size and the age of the gigantic landslides by drilling 300 km from Oahu where the units would be thin enough to achieve total penetration.

TECTONIC SETTINGS OF THE H2O AND NUUANU LANDSLIDE SITES

Hawaii-2 Observatory (Site 1224)

The H2O observatory is situated on oceanic lithosphere between the Murray and Molokai Fracture Zones within Isochron 20R (46.264 Ma) at ~140°W (Stephen, Kasahara, Acton, et al., 2003), avoiding the tectonically complicated region to the east and the fracture zone to the south. The observatory lies in the pelagic clay province of the North Pacific (Leinen, 1989). The sediments are reddish colored clays, mainly eolian in origin, consisting primarily of dust blown from Asia.

In more than 30 yr of deep ocean drilling prior to Ocean Drilling Program (ODP) Leg 200 and at more than 1200 sites worldwide, there had been only 13 holes with >10 m penetration into "normal" igneous Pacific plate. Among theses holes, only one was deeper than 100 m into basaltic basement, Deep Sea Drilling Project [DSDP] Leg 65 Hole 483B, and none of the holes were in crust with ages between 29 and 72 Ma.

At the latitude and age of the H2O area, the spreading rate was 142 mm/yr (full rate). Prior to drilling we thought that a reference station in "normal ocean," very fast spreading Pacific crust at 45–50 Ma would constrain geochemical and hydrothermal models of crustal evolution. Surprisingly, chemical analysis of the basalts obtained at Site 1224 showed far from the expected normal mid-oceanic-ridge basalt (N-MORB) characteristics, and it is difficult to say how the shallow part of the crust at the H2O site was formed.

Nuuanu Landslide (Site 1223)

Recent detailed bathymetric surveys have revealed the presence of huge landslides on the ocean floor, caused by volcanic eruptions in the Hawaiian Ridge (Moore et al., 1994), Reunion Island (Lenat et al., 1989), and the Canary Islands (Watts and Mason, 1995; Krasetel et al., 2001; Masson et al., 2002). It has been suggested that the gravitational instability of the volcanic edifices resulted in collapse. In the Canary Islands, the debris from the landslides extends to 30 km, and landslides on both island chains indicate generation of huge turbidity currents (Moore, 1964; Moore and Moore, 1988; Moore et al., 1989). In the case of Hawaii, the collapse of Koolau Volcano on Oahu caused the Nuuanu Landslide, which extends more than 200 km from the island (Fig. F2). The debris avalanche of the Nuuanu Landslide contains enormous blocks such as the Tuscaloosa Seamount, which is ~30 km long, 17 km wide, and at least 2 km thick. The Nuuanu Landslide is spread over a 23,000-km² area (Normark et al., 1993; Naka et al., 2000), with distal portions extending up onto the Hawaiian Arch. To reach the upper portion of the arch, the target site for drilling, the landslide would have had to traverse the deep moat on the northeast side of Oahu and travel more than 100 km uphill. Gravity and piston cores in the landslide are difficult to obtain because the deposit is overlain by a carapace of younger debris such as turbidites and associated deposits. Because of

such difficulties, the thickness and depositional history of the Nuuanu Landslide are poorly known. The thickness of the distal portion of the landslide was estimated to be 1–100 m based on seismic profiles (Rees et al., 1993) (Fig. F3). The upper 100 m of sediment at Site 1223 was thought to contain a record of the Nuuanu Landslide, a catastrophic event or series of events that removed ~40% (3000–4000 km^3) of Koolau Volcano on the island of Oahu (Herrero-Bervera et al., 2002; Normark et al., 1993). On the other hand, piston Core P3 in Figure F2 shows <1 m deposits from the Nuuanu slide (Naka et al., 2000). This ambiguity in the thickness of the Nuuanu sedimentary deposits creates a large uncertainty in the estimation of landslide volume. Although the Nuuanu Landslide apparently occurred near the end or after the formation of the Koolau Volcano, which has surface flows that are 1.8–2.7 Ma based on K-Ar dating (Doell and Dalrymple, 1973), the exact age of the landslide was not well constrained prior to drilling.

PREVIOUS DRILLING AND SEISMIC REFLECTION STUDIES

H2O (Site 1224)

During DSDP Leg 5, a series of holes (Sites 39–41) was drilled in the pelagic clay province along longitude 140°W (McManus, Burns, et al., 1970). Site 39 is located north of the Hawaii-2 cable at latitude 32°8.28′N with an age of 60 Ma, and the sediment thickness is only 17 m. Sites 40 and 41 are near the same latitude, at 19°0′N with an age of ~67 Ma. Site 39 is north of the Murray Fracture Zone, and Sites 40 and 41 are south of the Molokai Fracture Zone. The actual "ribbon" of crust on which the cable lies is between the two fracture zones and was not drilled during DSDP Leg 5. Site 40 was drilled in a sediment pond at the base of a large abyssal hill, and drilling was terminated at a chert bed at 156 meters below seafloor (mbsf). The acoustic basement identified as the deepest horizon in the reflection records corresponded to the chert beds. Site 41, located 15 km from Site 40, was considered to be more representative of the sediments in the general area. At this site, basaltic basement was found at 34 mbsf, but there were no cherts. DSDP Leg 18 Site 172 was located between the Murray and Molokai Fracture Zones but east of 140°W in the "disturbed" zone south of Moonless Mountain (Marmmerickx, 1989) (31°2.23′N, 133°2.36′W) at an estimated crustal age of 35 Ma (Kulm, von Huene, et al., 1973). At Site 172, sediment thickness above the basaltic basement was 24 m. The sediment thickness from seismic reflection profiles, however, had been interpreted as 90–105 m. The cause of this discrepancy was attributed to "reverberations in the sedimentary layer and thin sediment cover" (Stephen, Kasahara, Acton, et al., 2003).

Nuuanu (Site 1223)

During ODP Leg 136 (1991), two sites (Sites 842 and 843) were drilled into the western Hawaiian Arch ~250 km southwest of the island of Oahu (Fig. F2). At theses sites sand layers associated with turbidites from three major Hawaiian landslides were obtained. Quaternary to upper Eocene sediments were recovered to a depth of ~35 mbsf (Dziewonski, Wilkens, Firth, et al., 1992).

In 1998 and 1999, Japan Agency for Marine-Earth Science and Technology (JAMSTEC) cruises (Naka et al., 2000) made bathymetric surveys, dredges, and submersible dives and collected four piston cores targeting the Nuuanu Landslide field and the Wailau Landslides from nearby East Molokai Volcano (Takahashi et al., 2002). The seismic profile along Line 12 (Rees et al., 1993) is shown in Figure F3. Site 1223 is at the northeastern end of Line 12.

RESULTS OF DRILLING AT THE H2O SITE

Installation of a Reentry Cone and Casing at Site 1224 for a Future Borehole Seismometer Installation

The cased reentry hole (Hole 1224D), which is suitable for a broadband borehole seismometer installation, is located at 27°2.916′N, 141°9.504′W in 4979 m water depth, 1.48 km northeast of the H2O junction box. Until the downhole seismometer is properly installed, casing will act to stabilize the reentry cone. A reentry cone with 24 m of 20-in casing was installed by jetting-in. Suspended below the reentry cone is 58.5 m of 10.75-in casing, which was cemented into a 30-m-thick, well-consolidated, massive basalt flow underlying 28 m of soft, red clay.

Prior to installation of the 10.75-in casing, Hole 1224D was cored using the rotary core barrel (RCB) through the sediment/basement interface at ~28 mbsf and down through basaltic basement to a depth of 59 mbsf. We cored ~31 m of aphyric basalt with 15.7 m recovery. Basalts consist of several flows. In the upper part of the red clay layer, radiolarians are abundant. After RCB coring, we expanded the hole using a 14¾-in drill bit to 70 mbsf.

After preparing Hole 1224D for the borehole seismometer, we drilled a single-bit hole (1224F), to 174.5 mbsf to acquire sediment and basalt samples for shipboard and shore-based analysis as well as to run a logging program. Hole 1224F is <20 m southeast of Hole 1224D, and measurements in Hole 1224F can be used to infer the structure surrounding both holes. Since Leg 200, another cased reentry hole (Hole 1243A) suitable for a borehole seismometer was drilled during Leg 203 at 5°18.0541′N, 110°4.5798′W in the eastern Pacific (Orcutt, Schultz, Davies, et al., 2003).

Noise Spectra Observed by the H2O Shallow-Buried Broadband Seismometer during Leg 200

Amplitude-spectral characteristics of seismic signals could be affected by wind speed, sea state, shear resonance effects in the sediments, whales, air and/or water gun shooting, earthquakes, passing ships, and drilling-related activities such as bit noise and running pipe. Drilling-related noise from the *JOIDES Resolution* was observed in data collected by the shallowly buried seismometer (frequency band 0.01–80 Hz) being operated at the site by the University of Hawaii (Duennebier et al., 2002) (www.soest.Hawaii.edu/H2O/). Seismic data from the H2O observatory were acquired continuously from October 1999 until May 2003, and the data are available to scientists world-wide through the Incorporated Research Institutions for Seismology (IRIS) Data Management Center in Seattle. Drilling activities and sea bottom noise were well recorded by the H2O seismometers. During the operations,

weather and sea-state data were recorded. The comparison of seismic signals with local and distant weather and sea-state data has enabled us to better understand the behavior of double-frequency microseisms in the open ocean (Stephen et al., this volume; Bromirski et al., 2005).

Figure F4 shows spectrograms acquired during this period (Stephen et al., this volume). The spectrograms show very large noise levels from 0.1 to 1 Hz with a peak at ~0.2 Hz, especially on the horizontal components. Large noise levels also appear at frequencies <0.02 Hz and higher than ~30 Hz. In the frequency band between 0.02 and 0.1 Hz, noise levels are very small. In the open ocean the double-frequency microseism peak split into two peaks. Comparison of the ship weather log with seismic data from ~0.2 to 0.5 Hz shows a strong correlation between seismic amplitude and local wind speed, suggesting the seismic noise at the ocean floor in this band is generated by local weather at the sea surface (Bromirski et al., 2005). On the other hand, in the band 0.1–0.2 Hz, the noise correlates poorly with local weather, suggesting a long-distance source. Noise in this band seems to correlate with high sea states impinging on distant coastlines. Large quasi-periodic noise was also identified (Stephen, Kasahara, Acton, et al., 2003) and was surmised to be whales singing. Other noise sources were identified as drilling noise by coincidence with drilling activity (Stephen, Kasahara, Acton, et al., 2003). Overall noise spectra are shown in Figure F5.

Seismic Signature Observed by the 3.5-kHz Deep Source

A long-standing problem in the red clay province of the eastern Pacific is to adequately resolve chert layers and basement in the presence of sediments <50 m thick. During Leg 200 we lowered a battery-powered, free-running 3.5-kHz pinger to the seafloor on the vibration isolated television sled and recorded the pulse on the ship's 3.5-kHz acquisition system. This increased the sound level incident on the seafloor and improved penetration into the subbottom reduced the footprint of the sound on the seafloor and increased the received signal levels. Two prominent reflections were observed at ~10 mbsf (= 13 ms two-way traveltime [TWT]) and 28 mbsf (= 38 ms TWT), but the continuity of these reflectors varies with time throughout the survey, even though the ship moved only a few meters (Fig. F6) (Bolmer et al., this volume). The origin of the first subseafloor reflection at 10 mbsf could not be clearly identified in the core. V_P obtained by physical property measurements on the *JOIDES Resolution* shows gradually increasing velocities from 1.48 km/s at the ocean bottom to 1.50 km/s at 7 mbsf (Stephen, Kasahara, Acton, et al., 2003). The population of radiolarians increases toward 7 mbsf. This suggests that the 13-ms reflector may be a radiolarian abundant layer similar to one observed at the Barbados décollement (Moore et al., 1998; Moore, 2000). In Barbados, the décollement layer comprises a radiolarian layer with an abundance of fluid methane lodged in large cavities of the radiolarians. The depth of the second subseafloor reflector at 28 mbsf corresponds to basaltic basement.
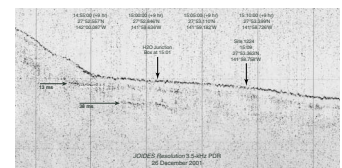
F4. Guralp component spectrograms, p. 21.
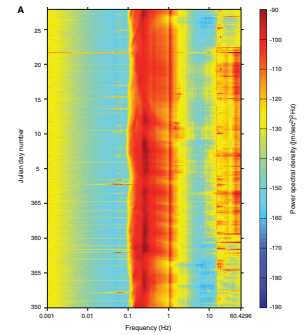
F5. Noise spectra obtained by the H2O, p. 23.
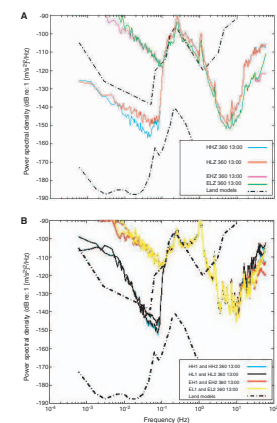
F6. 3.5-kHz seismic record, p. 24.

LITHOLOGICAL AND GEOCHEMICAL CHARACTERISTICS AND PHYSICAL PROPERTIES OF THE BASALTIC LAYER AT THE H2O SITE

We define lithologic units based on core analyses and logging results.

Lithological Characteristics

The total sediment thickness at Site 1224 is ~28–30 m (Fig. F7). Paleontological analysis of calcareous nannofossils suggests that the whole sedimentary sequence was deposited within a few million years of the crustal age of ~46 Ma (Eocene) or contains reworked Eocene radiolarians. Basement at Site 1224 is separated into three lithologic units: Unit L-1 (massive flows; 26–62.7 mbsf), Unit L-2 (thin flows and pillow basalts; 62.7–133.5 mbsf), and Unit L-3 (intermediate to thin flows and pillow basalts; 133.5 mbsf). Unit L-1 is divided into upper and lower flow units based on grain size of groundmass and distribution of alteration effects.

The lithologic unit boundaries were also identified by logging and physical property measurements. Logging Units LG-I and LG-II correspond to lithologic Unit L-1, logging Units LG-III and LG-IV correspond to lithologic Unit L-2, and logging Unit LG-V corresponds to lithologic Unit L-3.

Lithologic Unit L-1

Depth: 28–62.7 mbsf
Thickness: 34.7 m

The massive basalt flows of lithologic Unit L-1 are subdivided into upper and lower subunits. This unit includes all basalt cores of Holes 1224A, 1224D, and 1224E. The base of the unit in Hole 1224F is curated at 62.7 mbsf, and its thickness in Hole 1224F is curated at 34.7 m. Recovery in Unit L-1 was 52.6%. Logging data show changes in porosity and density at the curated depth of the base of Unit L-1.

Lithologic Unit L-2

Depth: 62.7–133.5 mbsf
Thickness: 70.8 m)

Changes in logging porosity and density corresponding to the base of Unit L-2 occur at ~140 mbsf, a few meters deeper than the curated depth. This lithologic unit comprises thin flows and two major pillow zones. The base of Unit L-2 is curated at 133.5 mbsf, and its thickness as curated is 70.8 m. Recovery in Unit L-2 was 14.6%. Two hyaloclastites were recovered in this unit.

Lithologic Unit L-3

Depth: 133.5–161.7 mbsf
Thickness: 28.2 m)

Lithologic Unit L-3 comprises basalt flows of intermediate thickness alternating with thin flows and pillows. The base of the unit is at 161.7

F7. Core description, Site 1224, p. 25.
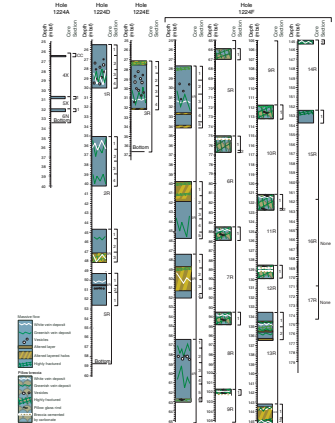
mbsf, and its curated thickness is 28.2 m. Recovery in Unit L-3 was 21.4%.The changes in physical properties and downhole logging data correspond to the lithologic and chemostratigraphic changes that define the units and subunits.

Geochemical Characteristics of the Basement Drilled on the Pacific Plate

Geochemical analysis shows important results (Haraguchi and Ishii, this volume; Lustrino, this volume) (Fig. F8A). SiO_2 is distributed at 48–53 wt% and MgO at 5–7 wt%. FeO/MgO ratio characteristics of the rocks from all three units are 1.3–3.0, higher than the typical MORB ratio (normally 1–1.5). Some lavas in the core have the highest iron enrichment differentiation among abyssal tholeiites in the eastern Pacific. FeO and TiO_2 are as high as ~14 wt% and 3.5 wt%, respectively (Fig. F8A, F8B) (Haraguchi and Ishii, this volume). Those basalts are altered differentiated tholeiitic ferrobasalts with the depleted geochemical characteristics of MORB. High FeOT and TiO_2 were found in Hole 735B in the southwestern Indian Ocean (e.g., Dick et al., 2002), at Juan de Fuca Ridge, and recently in Atlantis massif during Integrated Ocean Drilling Program (IOPD) Expedition 304/305 (Ohara et al., 2005). These materials are classified as ferrobasalts (e.g., Natland, 1980) and/or ferrogabbro. Incompatible element analysis of three basement rocks show high contents, a factor of 2 or more of high field strength element (HFSE; Y and Zr) content than N-MORB, and some element contents are similar to ocean island basalt (OIB) as complied by Sun and McDonough (1989) (Haraguchi and Ishii, this volume). The depth dependences of Nb, Y, and Zr are very similar to the TiO_2 distribution (see Fig. F8C) (Lustrino, this volume). Y is a factor of 2 greater than OIB, and the Y/Zr ratio is similar to that of normal and enriched MORB in contrast to that of OIB (Fig. F9). Differences in HFSE and rare earth element compositions among the three units are remarkable. Lithologic Unit L-2 is subdivided into two characteristic layers by similar incompatible elements. Lithologic Unit L-3 has high contents of these elements and Unit L-2 has low. Unit L-3 pillows show almost the greatest TiO_2 enrichment (Fig. F8B) (Lustrino, this volume), as observed elsewhere along the East Pacific Rise (Natland, 1991) and corresponds to the highest end of the differentiation process.

Paul et al. (2006) analyzed the alteration at this site and found that most of the basalts are <5% altered to secondary mineral assemblages of Fe oxyhydroxides, celeadonite, saponite, Ca carbonate, trace pyrite, and rare phillipsite and quartz. They also found that Ca carbonate formed within 20 m.y. of crustal formation and occurred at low temperatures (4°–11°C).

## Logging and Physical Property Characteristics

Logging by two wireline tool strings was carried out in Hole 1224F. Using both drilling and logging data, we can make an excellent comparison of the petrological and geophysical characteristics of upper basaltic layers in fast-spreading Pacific crust at an age of ~46 Ma.

The triple combination (triple combo) tool string (Accelerator Porosity Sonde [APS], Hostile Environmental Litho-Density Tool [HLDT], and Dual Induction Tool [DIT]) was used for the first logging run. A tool string consisting of the Formation MicroScanner [FMS], General Pur-

F8. Distribution of chemical elements, p. 26.
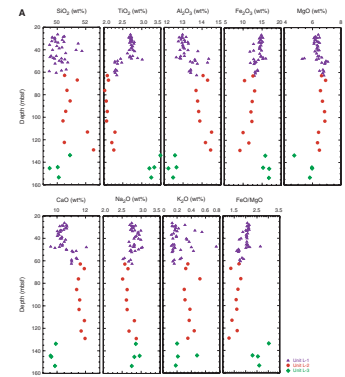
F9. Y vs. Zr, Hole 1224F, p. 29.
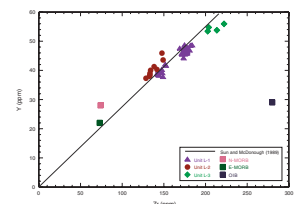
pose Inclinometer [GPIT], and Dipole Sonic Imager [DSI] was used for the second logging run. Five physical parameters (density, porosity, V_P, V_S, and magnetic susceptibility) were obtained during logging (Figs. F10, F11). For the layer unit classification based on logging, we use LG. In Hole 1224F, we can identify five distinct basaltic logging units in the basement below the ~28-m-thick sediment layer (Fig. F10):

28–45 mbsf (logging Unit LG-I),
45–63 mbsf (logging Unit LG-II),
63–103 mbsf (logging Unit LG-III),
103–142 mbsf (logging Unit LG-IV), and
Deeper than 142 mbsf (logging Unit LG-V).

The temperature in the hole also increases at 135–137 mbsf, suggesting that seawater flowing down the hole entered the formation in a zone of high permeability at this depth.

On the other hand, P-wave velocities from core samples acquired by the shipboard scientific party (Stephen, Kasahara, Acton, et al., 2003) identified seven layers (Table T1) at 38, 41, 65, 100, 132, 143, and below 143 mbsf, shown in Figures F11 and F12. Except for two thin layers, the rest of the layer boundaries are nearly the same as the logging unit classification.

The comparison of logging data and physical properties for porosity, density, V_P, and V_S is shown in Figure F13. The two data sets fit well except for some porosity data in logging Units LG-III and LG-IV.

V_P and V_S measurements of 11 samples taken from Holes 1224D and 1224F under pressure up to 100 MPa do not show much change: 2.1% (5.6–5.72 km/s) for V_P and 3.6% (3.08–3.19 km/s) for V_S (Fig. F14) (Sun et al., this volume). The porosity of these samples is <5%. The shallow part of the oceanic crust usually shows sharp increases from 4.5 to 6.5 km/s, corresponding to the transition from Layer 2B to 2C or 3. Because velocity measurements under high pressure do not show a large velocity change, the velocity increase observed in the shallow oceanic crust may be caused by a change from the fracture-altered basalts to massive, less fractured basalts. Macroscopic porosities can be produced by fractures because basalt specimens do not show extremely high porosities.

A seismic model down to 170 mbsf was obtained based on velocities from physical properties measurements and logging (Fig. F15). It will aid the analysis of the broadband, downhole seismometer data. Sun et al. (this volume) produced synthetic seismograms using logging V_P values (Fig. F16). They compared the synthetic waveforms with the seismic reflection records and obtained good agreement (Fig. F17). Based on the reflection records (Stephen, Kasahara, Acton, et al., 2003) (Fig. F18), there is a deeper reflector at 60 ms TWT. This deeper reflector corresponds to the unit boundary at ~137–143 mbsf between logging Units LG-IV and LG-V or synthesis Unit S-6. In Leg 148 Hole 504B in the Panama Basin, the highly fractured zone was found at ~600–800 mbsf (Alt, Kinoshita, Stokking, et al., 1993). Average porosities in synthesis Unit S-5 are ~20%–60%. Porosities in synthesis Unit S-6 are 50%. Units S-1 through S-3 also show porosities of 40%–70%.

Recently, very intensive seismic surveys using a large number of ocean bottom seismometers and >8000-in³ air guns have been carried out (e.g., Nishizawa et al., 2005a, 2005b; Kaneda et al., 2005). The tomographic and forward analyses of traveltimes and waveforms show that the velocity profiles in the upper crust are not well resolved be-
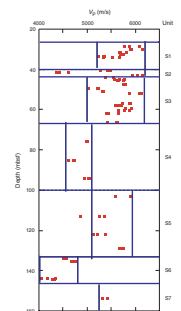
F10. Physical properties, Hole 1224F, p. 30.
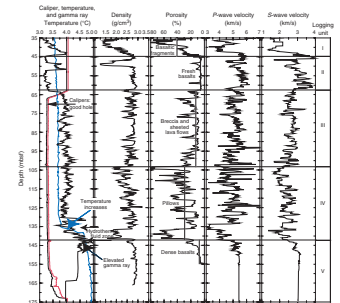
F11. Logging data and synthesis units, Hole 1224F, p. 31.
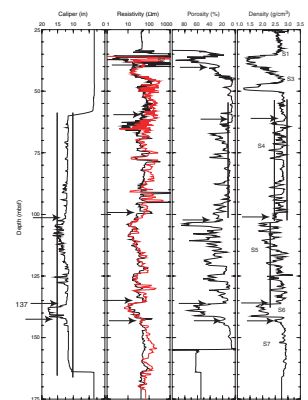
T1. Synthesis units, p. 44.

F12. P-wave velocities and synthesis units, Hole 1224F, p. 32.

cause ray paths are masked by water waves, in particular, when the high-velocity layer is near the ocean floor. Therefore, the present result is one of a few good models for the uppermost part of oceanic crust. The present results can be used to make a receiver function model for the downhole seismometers.

## Comparison of Physical Properties, Logging, and Geochemistry

Logging data and physical property data may mainly relate to the mechanical properties, but lithological and geochemical measurements may mainly relate to the results of chemical reaction and alteration. Table T1 summarizes synthesis units (S-0 through S-7), distinguished mainly based on physical properties. There is excellent agreement among physical properties, logging, lithological, and geochemical data. Physical property measurements (Stephen, Kasahara, Acton, et al., 2003) suggest that synthesis Units S-3 through S-6 (Table T1) are largely fractured. Rock samples from synthesis Units S-1 through S-7 contain large amounts of altered minerals in halos (Paul et al., 2006). V_P in synthesis Units S-2 and S-6 is lower than other units (4.0–4.5 km/s). For these two units, alteration and microfractures penetrate into small rock bodies (Fig. F11). Especially, V_P in synthesis Unit S-6 is the lowest among the measured V_P. The percentage in halos in synthesis Unit-S6 is higher than other synthesis units (Paul et al., 2006). The abrupt change of water temperature in synthesis Unit S-6 is related to water flow through fractures suggested by this high percentage.

Microbiological Studies in Basalts

Recently, a huge amount of biomass has been found living in the extreme conditions found under the seafloor (e.g., Isozaki et al., 2003). Prokaryotes significantly contribute to the overall biomass in marine ecosystems and play a major role in biogeochemical processes (Nealson, 1997; Parkes et al., 2000; Newman and Banfield, 2002). To date, prokaryotes have dominated the discoveries of microbial life in deeply buried oceanic sediments (Parkes et al., 1994) and sedimentary rocks (Lovley and Chapelle, 1995; Zhang et al., 1997; Liu et al., 1997). Microorganisms have been recovered from depths as deep as 800 mbsf in sediment (Taylor, Huchon, Klaus, et al., 1999) and have been found fossilized within continental basalts of the Columbia River basalts group (McKinley et al., 2000). Based on previous studies, it is thought that eukaryotes are less likely to be found in extreme environments such as subseafloor sediment and rocks.

Using standard optical microscopic techniques and field emission scanning electron microscopy (FE-SEM) with an X-ray energy dispersed (EDX) spectrometer system, dark brownish filamentous structures within carbonate-filled vesicles (0.3–3 mm in diameter) were found in Hole 1224D. These were analyzed and were interpreted to be fossilized fungi based on morphological traits including branching, septa, and central pores (Schumann et al., 2004) (Fig. F19). Schumann et al. (2004) proposed that these represent higher anaerobic fungi because they have septated hyphae. Chemical analysis shows that the chemical composition of the fungal structure differs from the surrounding crystalline carbonate matrix. The discovery of fungal eukaryotes in abyssal basalts is surprising because micro-eukaryotes are thought to live in the subsur-
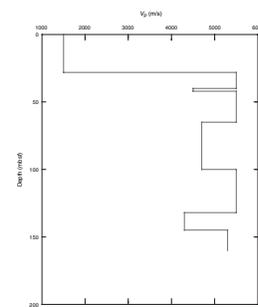
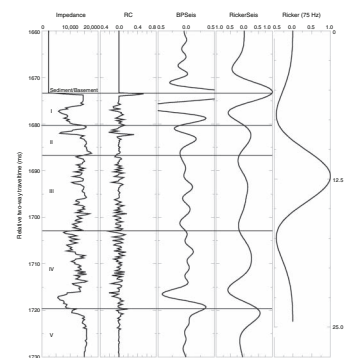**F13.** Logging and shipboard physical properties, p. 33.
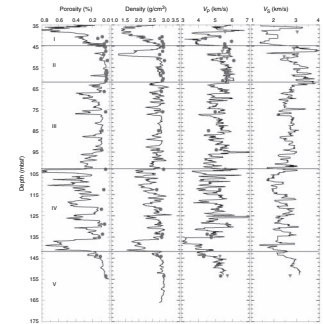
F14. V_P and V_S under pressure to 100 MPa, p. 34.
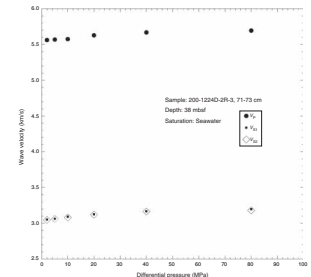
F15. V_P estimated using shipboard physical properties, p. 35.

F16. Synthetic seismogram using logging V_P and density, p. 36.

face only in aquifers with relatively young groundwater (Balkwill, 1989).

RESULTS AT THE NUUANU LANDSLIDE SITE

Hole 1223A, the Nuuanu site (22°58.4095′N, 155°39.2590′W, water depth = 4235.1 m), was drilled to 41 mbsf. The advanced piston corer (APC) was used for depths shallower than 12.7 mbsf. At this depth, indurated sediments were encountered and the drilling system was switched to the extended core barrel (XCB). Figure F20 shows the core description (Garcia et al., 2006). Two types of major lithological layers are found: fine-grained clay and silt layers and volcanic sand layers. Sediments shallower than 12.7 mbsf are unconsolidated. Deeper in the hole there are weakly consolidated fine-grained sediments and indurated sands that are estimated to be volcaniclastic sandstones. Above 12.7 mbsf, six unconsolidated sand layers (sand Layers 1–6) were identified. Below 12.7 mbsf two volcanic sandstones and several volcaniclastic claystone units were identified (Stephen, Kasahara, Acton, et al., 2003). A part of the upper sandstone was lost during APC drilling (sand Layer 7 in Fig. F20). The thickness is unknown. The sandstone is moderately indurated and normally size graded with angular to subrounded fragments of fresh glass, minerals, and vitric and lithic clasts in a radiolarian-bearing clayey matrix.

At 32 mbsf, lower sandstone (sand Layer 8) was encountered. The upper part of sand Layer 8 is poorly consolidated and highly disturbed. The lower part is well lithified. Characteristics of the lower sandstone (sand Layer 8) are similar to those of the upper (sand Layer 7) except for the more advanced stage of glass alteration (Garcia et al., 2006).

Results of physical property measurements are presented in Figures F21 and F22. Units are as described in the Leg 200 *Initial Results* volume (Stephen, Kasahara, Acton, et al., 2003). Sand layers shallower than 12.7 mbsf are unconsolidated and have correspondingly low V_P (~1.7 km/s). Among the sand layers, V_P and density oscillate, indicating graded bedding in the sand layers. Deeper than 12.7 mbsf, V_P drastically increases to >3.3 km/s, suggesting induration of the sand layers. Some specimens, however, show V_P between 1.8 and 2.4 km/s, which corresponds to clayey layers. The deepest sand layer (sand Layer 8 in Fig. F20) at ~35 mbsf shows V_P of ~4 km/s, indicating induration. These physical property measurements are consistent with lithological studies.

Radiolarians were found in layers at 3.02–3.9 and 5.10–6.70 mbsf. The shallower layer suggests that sand Layers 1–3 were emplaced in the Neogene. Radiolarians in the deeper sand Layer 6 give an Eocene age, suggesting collapse and reworking of the older sediments. Radiolarian studies from several intervals in the cores yield ages ranging from Quaternary to early Eocene, indicating that the turbidity currents that deposited the sand eroded older sediments around the Hawaiian Islands (Garcia et al., 2006; Popova-Goll and Goll, this volume).

A magnetostratigraphic study shows that Site 1223 cores are dated from Chron C1n (0–0.78 Ma) to Chron 2r (1.95–2.581 Ma). Chron 1r.1n (0.99–1.07 Ma) appears from 0.80 to 1.23 mbsf, and Chron C2n extends from 2.02 to 7.19 mbsf. Below 7.19 mbsf, the section is interpreted to be entirely reversed polarity and is estimated to have been deposited within Chron C2r (1.95–2.58 Ma) (Garcia et al., 2006).

Sand layers contain abundant basalt detritus including fresh glass, olivine, and plagioclase fragments. Sand Layer 1 is distinct from the other
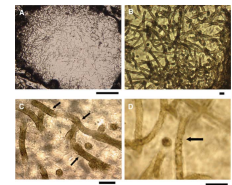
F17. Comparison of seismic reflections with synthetic seismograms, p. 37.
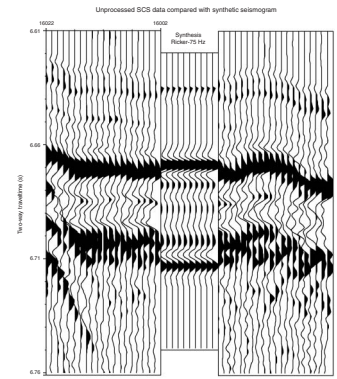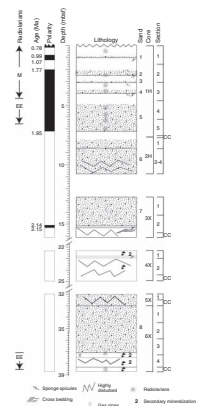

F18. Seismic reflection record and interpretation using synthetic seismograms, p. 38.
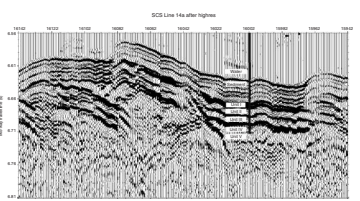
F19. Filamentous fungal structures in basalt, p. 39.

F20. Lithologic units, Hole 1223A, p. 40.

sand layers, with abundant rock fragments and sparse glass. The other sand layers have abundant glass. The indurated volcaniclastic sandstones are petrographically similar to unconsolidated sand layers except for their more advanced stages of alteration and lithification and the presence of zeolites in voids (Garcia et al., 2006).
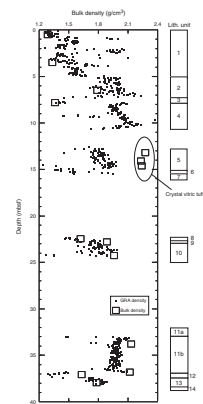
The composition of the glass sands was determined by microprobe. More than 800 samples were analyzed; they are all tholeiitic and typical of Hawaiian shield volcanoes (Fig. F23) (Garcia et al., 2006). MgO contents are distributed at 6–8 wt%, the common range for Hawaiian tholeiitic glasses (e.g., Clague et al., 1995; Davies et al., 2003). Three glasses in sand Layer 2 show unusually high MgO (up to 12.3 wt%), suggesting relatively primitive magma compositions and high quenching temperature (~1290°C). Sulfur contents are low (>0.03 wt%), suggesting subaereal eruption.

SUMMARY

Two sites were drilled during ODP Leg 200: the H2O site (Site 1224) and the Nuuanu Landslide site (Site 1223). Results are summarized as follows:

1. In Hole 1224D we drilled basaltic basement to 59 mbsf and installed a reentry cone with cemented casing for future installation of a borehole broadband seismometer.
2. During the H2O operations, broadband seismometer records obtained from the shallowly buried H2O seismometer were analyzed. In the midocean, the double-frequency microseism peak splits into two peaks associated with two different kinds of noise sources. Microseism levels in the band ~0.2–0.5 Hz correlated with sea state and wind speed observed from the drillship, indicating that this noise is generated locally at the sea surface. Microseism levels in the band 0.1–0.2 Hz correlate with high sea states impacting distant shorelines. Large quasi-periodic noises generated by whales and drilling-related noise were also identified.
3. Hole 1224F, 20 m away from Hole 1224D, was drilled to 173.5 mbsf. Drilling in Hole 1224F recovered >100 m of ~46-Ma basaltic basement that is composed of three units. Although these three units are geochemically distinct, they are more highly evolved than most MORB (i.e., they have experienced a protracted history of cooling and crystal fractionation within the crust).
4. Analysis of the alteration at this site showed that most of basalts are <5% altered to secondary minerals assemblages of Fe oxyhydroxides, celeadonite, saponite, Ca carbonate, trace pyrite, and rare phillipsite and quartz. Ca carbonate formed within 20 m.y. of crustal formation and occurred at low temperatures (4°–11°C).
5. Logging and physical property measurements show good correlation to lithology, geochemisty, and alteration of minerals in basalt. The fractures and low-temperature alteration greatly reduce V_P, suggesting a cause of V_P ~ 4.5 km/s in oceanic Layer 2B.
6. The discovery of fungi in calcite veins in abyssal basalts was made by microbiological analyses. This is evidence that eukaryotic life existed in the extreme environment below the seafloor.
7. The Nuuanu Landslide site, ~260 km northeast of the island of Oahu near the crest of the 500-m-high Hawaiian Arch, was also
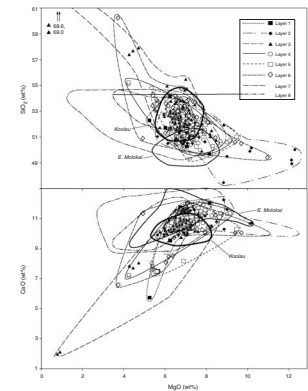
drilled. We drilled to 41 mbsf and identified eight sandy layers. The layers contain fresh and angular glass fragments typical of Hawaiian shield volcanoes. Degassed glasses are estimated to be subaerially erupted. Seven of the sandy layers are thought to be associated with the Koolau Landslide prior to 1.77 Ma. Of the four thicker sandy layers, it is unclear which are related to the Nuuanu Landslide. Analysis of the Site 1223 cores suggests repeated occurrences of collapsing Hawaiian volcanoes and debris flows to ~260 km distance.

ACKNOWLEDGMENTS

REFERENCES

Alt, J.C., Kinoshita, H., Stokking, L.B., et al., 1993. *Proc. ODP, Init. Repts.,* 148: College Station, TX (Ocean Drilling Program).

Balkwill, D.L., 1989. Numbers, diversity and morphological characteristics of aerobic chemoheterotrophic bacteria in deep subsurface sediments from a site in South Carolina. *Geomicrobiol. J.,* 7:33–52.

Bromirski, P.D., Duennebier, F.K., and Stephen, R.A., 2005. Mid-ocean microseisms. *Geochem., Geophys., Geosyst.,* 6(4):Q04009. **doi:10.1029/2004GC000768**

Clague, D.A., Moore, J.G., Dixon, J.E., and Friesen, W.B., 1995. Petrology of submarine lavas from Kilauea's Puna Ridge, Hawaii. *J. Petrol.,* 36:299–349.

Davies, M.G., Garcia, M.O., and Wallace, P., 2003. Volatiles in Mauna Loa glasses: implications for magma degassing and contamination, and growth of Hawaiian volcanoes. *Contrib. Mineral. Petrol.,* 144:570–591.

Dick, H.J.B., Ozawa, K., Meyer, P.S., Niu, Y., Robinson, P.T., Constantin, M., Hebert, R., Maeda, J., Natland, J.H., Hirth, J.G., and Mackie, S.M., 2002. Primary silicate mineral chemistry of a 1.5-km section of very slow spreading lower ocean crust: ODP Hole 735B, Southwest Indian Ridge. *In* Natland, J.H., Dick, H.J.B., Miller, D.J., and Von Herzen, R.P. (Eds.), *Proc. ODP, Sci. Results,* 176, 1–61 [Online]. Available from World Wide Web: **http://www-odp.tamu.edu/publications/176_SR/VOL-UME/CHAPTERS/SR176_10.PDF.**

Doell, R.R., and Dalrymple, G.B., 1973. Potassium-argon ages and paleomagnetism of the Waianae and Koolau Volcanic Series, Oahu, Hawaii. *Geol. Soc. Am. Bull.,* 84:1217–1242.

Duennebier, F.K., Harris, D.W., Jolly, J., Babinec, J., Copson, D., and Stiffel, K., 2002. The Hawaii-2 Observatory seismic system. *IEEE J. Oceanic Eng.,* 27:212–217. **doi:10.1109/JOE.2002.1002475**

Dziewonski, A., Wilkens, R., Firth, J., et al., 1992. *Proc. ODP, Init. Repts.,* 136: College Station, TX (Ocean Drilling Program).

Garcia, M.O., Sherman, S.B., Moore, G.F., Goll, R., Popova-Goll, I., Natland, J.H., and Acton, G., 2006. Frequent landslides from Koolau Volcano: results from ODP Site 1223. *J. Volcanol. Geotherm. Res.,* 151(1–3):251–268. **doi:10.1016/j.jvol-geores.2005.07.035**

Herrero-Bervera, E., Cañon-Tapia, E., Walker, G.P.L., and Guerrero-Garcia, J.C., 2002. The Nuuanu and Wailau giant landslides: insights from paleomagnetic and anisotropy of magnetic susceptibility (AMS) studies. *Phys. Earth Planet. Inter.,* 129(1–2):83–98. **doi:10.1016/S0031-9201(01)00238-2**

Isozaki, Y., Kasahara, J., and Toriumi, M. (Eds.), 2003. Life on the Earth: its origin and relevant extreme environments. *J. Geogr.,* 112:185–322.

Kaneda, K., Nishizawa, A., Katagiri, Y., and Kasahara, J., 2005. Crustal structure model of the Ogasawara Plateau colliding with the Philippine Sea plate [Joint Meeting for Earth and Planetary Science, 22–27 May 2005, Chiba, Japan], J028–011. (Abstract)

Kasahara, J., Utada, H., Sato, T., and Kinoshita, H., 1998. Submarine cable OBS using a retired submarine telecommunication cable: GeO-TOC program. *Phys. Earth Planet. Inter.,* 108(2):113–127. **doi:10.1016/S0031-9201(98)00090-9**

Kasahara, J. (Ed.), 2000. *Final Report of the VENUS Project:* Tokyo (Earthquake Research Inst.). (in Japanese)

Kasahara, J., Kawaguchi, K., Iwase, R., Shirasaki, Y., Kojima, J., and Nakatsuka, T., 2001. Installation of the multi-disciplinary VENUS observatory at the Ryukyu trench using Guam-Okinawa geophysical submarine cable, (GOGC: former TPC-2 cable). *JAMSTEC J. Deep Sea Res.,* 18:193–207.

Kasahara, J., Iwase, R., Nakatsuka, T., Nagaya, K., Shirasaki, Y., Kawaguchi, K., and Kojima, J., 2003. Multi-disciplinary VENUS observation at the Ryukyu Trench using Guam-Okinawa geophysical submarine cable. In *Proceedings of the Third Inter-*

national Workshop on Scientific Use of Submarine Cables and Related Technologies, 25–30.

Krasetel, S., Schmincke, H.-U., Jacobs, C.L., Rihm, R., Le Bas, T.P., and Alibes, B., 2001. Submarine landslides around Canary Island. *J. Geophys. Res.,* 106(B3):3977–3998. doi:10.1029/2000JB900413

Kulm, L.D., von Huene, R., et al., 1973. *Init. Repts. DSDP,* 18: Washington (U.S. Govt. Printing Office).

Leinen, M., 1989. The pelagic clay province of the North Pacific Ocean. *In* Winterer, E.L., Hussong, D.M., and Decker, R.W. (Eds.), *The Geology of North America* (Vol. N): *The Eastern Pacific Ocean and Hawaii.* Geol. Soc. Am., 323–335.

Lenat, J.-F., Vincent, P., and Bachelaery, P., 1989. The offshore continuation of an active basaltic volcano: Piton de la Fournaise (Réunion Island, Indian Ocean): structural and geomorphological interpretation from sea beam mapping. *J. Volcanol. Geotherm. Res.,* 36:1–9. doi:10.1016/0377-0273(89)90003-6

Liu, S.V., Zhou, J., Zhang, C., Cole, D.R., Gajdaziska-Josifovska, M., and Phelps, T.J., 1997. Thermophilic Fe(III)-reducing bacteria from the deep subsurface: the evolutionary implications. *Science,* 277(5329):1106–1109. doi:10.1126/science.277.5329.1106

Lovley, D.R., and Chapelle, F.H., 1995. Deep subsurface microbial processes. *Rev. Geophys.,* 33(3):365–381. doi:10.1029/95RG01305

Masson, D.G., Watts, A.B., Gee, M.J.R., Urgeles, R., Mitchell, N.C., Le Bas, T.P., and Canals, M., 2002. Slope failures on the flanks of the western Canary Islands. *Earth-Sci. Rev.,* 57(1–2):1–35. doi:10.1016/S0012-8252(01)00069-1

Mammerickx, J., 1989. Large-scale undersea features of the northeast Pacific. *In* Winterer, E.L., Hussong, D.M., and Decker, R.W. (Eds.), *The Eastern Pacific Ocean and Hawaii.* Geol. Soc. Am., Geol. of North Am. Ser., N:5–13.

McKinley, J.P., Stevens, T.O., and Westall, F., 2000. Microfossils and paleoenvironments in deep subsurface basalt samples. *Geomicrobiol. J.,* 17(1):43–54. doi:10.1080/014904500270486

McManus, D.A., Burns, R.E., et al., 1970. *Init. Repts. DSDP,* 5: Washington (U.S. Govt. Printing Office).

Moore, G.W., and Moore, J.G., 1988. Large scale bedforms in boulder gravel produced by giant waves in Hawaii. *In* Clifton, H.E. (Ed.), *Sedimentologic Consequences of Convulsive Geologic Events.* Spec. Pap.—Geol. Soc. Am., 229:101–109.

Moore, J.C., Stauffer, P.H., Teas, P.A., Klaus, A., Bangs, N.L., Bekins, B., Bücker, C.J., Brückmann, W., Erickson, S.N., Hansen, O., Horton, T., Ireland, P., Major, C.O., Moore, G.F., Peacock, S., Saito, S., Screaton, E.J., Shimeld, J.W., Taymaz, T., and Tokunaga, T., 1998. Consolidation patterns during initiation and evolution of a plate-boundary décollement zone: northern Barbados accretionary prism. *Geology,* 26(9):811–814. doi:10.1130/0091-7613(1998)026<0811:CPDIAE>2.3.CO;2

Moore, J.C., 2000. Synthesis of results: logging while drilling, northern Barbados accretionary prism. *In* Moore, J.C., and Klaus, A. (Eds.), *Proc. ODP, Sci. Results,* 171A: College Station TX (Ocean Drilling Program), 1–25. [PDF]

Moore, J.G., 1964. Giant submarine landslides on the Hawaiian Ridge. *Geological Survey Research 1964.* U.S. Geol. Surv. Prof. Pap., 501-D:95–98.

Moore, J.G., Clague, D.A., Holcomb, R.T., Lipman, P.W., Normark, W.R., and Torresan, M.E., 1989. Prodigious submarine landslides on the Hawaiian Ridge. *J. Geophys. Res.,* 94:17465–17484.

Moore, J.G., Normark, W.R., and Holcomb, R.T., 1994. Giant Hawaiian landslides. *Annu. Rev. Earth Planet. Sci.,* 22(1):119–144. doi:10.1146/annurev.ea.22.050194.001003

Naka, J., Takahashi, E., Clague, D., Garcia, M., Hanyu, T., et al., 2000. Tectono-magmatic processes investigated at deep-water flanks of Hawaiian volcanoes. *Eos, Trans. Am. Geophys. Union.,* 81:227–230.

Natland, J.H., 1980. Effect of axial magma chambers beneath spreading centers on the compositions of basaltic rocks. *In* Rosendahl, B.R., Hekinian, R., et al., *Init. Repts. DSDP,* 54: Washington (U.S. Govt. Printing Office), 833–850.

Natland, J.H., 1991. Indian Ocean crust. *In* Floyd, P.A. (Ed.), *Oceanic Basalts:* Glasgow (Blackie), 288–310.

Nealson, K.H., 1997. Sediment bacteria: who's there, what are they doing, and what's new? *Annu. Rev. Earth. Planet. Sci.,* 25:403–434.

Newman, D.K., and Banfield, J.F., 2002. Geomicrobiology: how molecular-scale interactions underpin biogeochemical systems. *Science,* 296(5570):1071–1077. **doi:10.1126/science.1010716**

Nishizawa, A., Kaneda, K., Katagiri, Y., and Kasahara, J., 2005a. Crustal structure around the Oki-Daito Ridge in the northern west Philippine Basin [Joint Meeting for Earth and Planetary Science, 22–27 May 2005, Chiba, Japan], J028-004. (Abstract)

Nishizawa, A., Kaneda, K., Katagiri, Y., and Kasahara, J., 2005b. Crustal structure across the southern Kyushu-Palau Ridge in the Philippine Sea [Joint Meeting for Earth and Planetary Science, 22–27 May 2005, Chiba, Japan], J028-006. (Abstract)

Normark, W.R., Moore, J.G., and Torresan, M.E., 1993. Giant volcano-related landslides and the development of the Hawaiian Islands. *In* Schwab, W.C., Lee, H.J., and Twichell, D.C. (Eds.), *Submarine Landslides: Selected Studies in the U.S. Exclusive Economic Zone.* U.S. Geol. Surv. Bull., 2002:184–196.

Ohara, Y., Abe, N., Andal, E.S., Awaji, S., Hirose, T., et al., 2005. Drilling at Atlantis Massif oceanic core complex: IODP Expedition 304/305 [Joint Meeting for Earth and Planetary Science, 22–27 May 2005, Chiba, Japan], J078-005. (Abstract)

Orcutt, J.A., Schultz, A., Davies, T.A., et al., 2003. *Proc. ODP, Init. Repts.,* 203 [CD-ROM]. Available from: Ocean Drilling Program, Texas A&M University, College Station TX 77845-9547, USA. [**HTML**]

ORION, 2004. A report of the workshop held January 4–8, 2004, San Juan, Puerto Rico. Available from the World Wide Web: **http://www.geo-prose.com/projects/orion_report.html.**

Parkes, R.J., Cragg, B.A., Bale, S.J., Getliff, J.M., Goodman, K., Rochelle, P.A., Fry, J.C., Weightman, A.J., and Harvey, S.M., 1994. Deep bacterial biosphere in Pacific Ocean sediments. *Nature (London, U. K.),* 371(6496):410–413. **doi:10.1038/371410a0**

Parkes, R.J., Cragg, B.A., and Wellsbury, P., 2000. Recent studies on bacterial populations and processes in subseafloor sediments: a review. *Hydrogeol. J.,* 8(1):11–28. **doi:10.1007/PL00010971**

Paul, H.J., Gillis, K.M., Coggon, R.M., and Teagle, D.A.H., 2006. ODP Site 1224: a missing link in the investigation of seafloor weathering. *Geochem., Geophys., Geosyst.,* 7(2). **doi:10.1029/2005GC001089**

Rees, B.A., Detrick, R.S., and Coakley, B.J., 1993. Seismic stratigraphy of the Hawaiian flexural moat. *Geol. Soc. Am. Bull.,* 105:189–205.

Schumann, G., Manz, W., Reitner, J., and Lustrino, M., 2004. Ancient fungal life in north Pacific Eocene oceanic crust. *Geomicrobiol. J.,* 21(4):241–246. **doi:10.1080/01490450490438748**

Stephen, R.A., Kasahara, J., Acton, G.D., et al., 2003. *Proc. ODP, Init. Repts.,* 200 [CD-ROM]. Available from: Ocean Drilling Program, Texas A&M University, College Station TX 77845-9547, USA. [**HTML**]

Stephen, R.A., Spiess, F.N., Collins, J.A., Hildebrand, J.A., Orcutt, J.A., Peal, K.R., Vernon, F.L., and Wooding, F.B., 2003. Ocean seismic network pilot experiment. *Geochem., Geophys., Geosyst.,* 4(10):1092. **doi:10.1029/2002GC000485**

Sun, S.-S., and McDonough, W.F., 1989. Chemical and isotopic systematics of oceanic basalts: implications for mantle composition and processes. *In* Saunders, A.D., and Norry, M.J. (Eds.), *Magmatism in the Ocean Basins.* Geol. Soc. Spec. Publ., 42:313–345.

Takahashi, E., Lipman, P.W., Garcia, M.O., Naka, J., and Aramaki, S. (Eds.), 2002. *Hawaiian Volcanoes: Deep Underwater Perspectives.* Geophys. Monogr., 128:418.

Taylor, B., Huchon, P., Klaus, A., et al., 1999. *Proc. ODP, Init. Repts.,* 180 [Online]. Available from World Wide Web: http://www-odp.tamu.edu/publications/180_IR/180TOC.HTM.

Watts, A.B., and Masson, D.G., 1995. A giant landslide on the north flank of Tenerife, Canary Islands. *J. Geophys. Res.,* 100(B12):24487–24498. doi:10.1029/95JB02630

Zhang, C., Shi, L., Phelps, T.J., Cole, D.R., Horita, J., Fortier, S.M., Elless, M., and Valley, J.W., 1997. Physiochemical, mineralogical, and isotopic characterization of magnetite-rich iron oxides formed by thermophilic iron-reducing bacteria. *Geochim. Cosmochim. Acta.,* 61(21):4621–4632. doi:10.1016/S0016-7037(97)00257-3

Figure F1. Location map of drilling sites during Leg 200 and Hawaii-2 submarine cable. Line 12 is also shown (Rees et al., 1993). FZ = fracture zone.
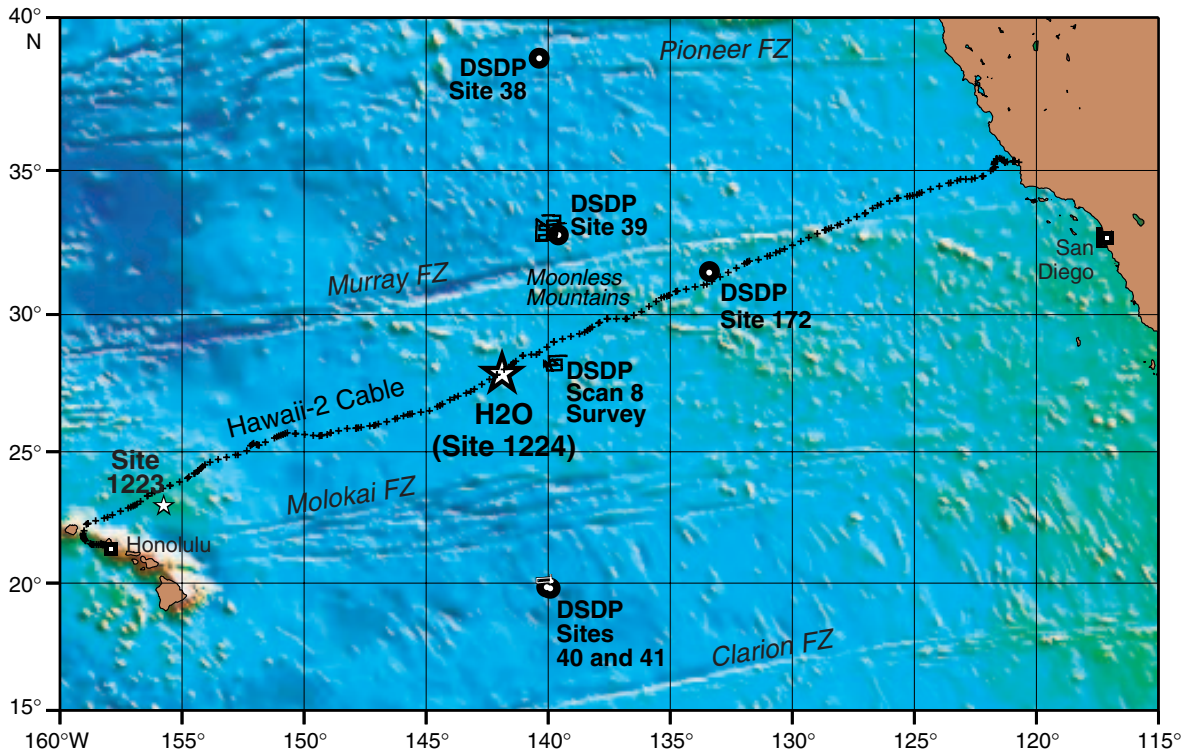
Figure F2. Nuuanu Landslide north of Oahu, Hawaii, piston Cores P1–P3, and seismic reflection records along Line 12 from Rees et al. (1993) collected by the 1998 *Thomas Washington* cruise (Garcia et al., 2006).
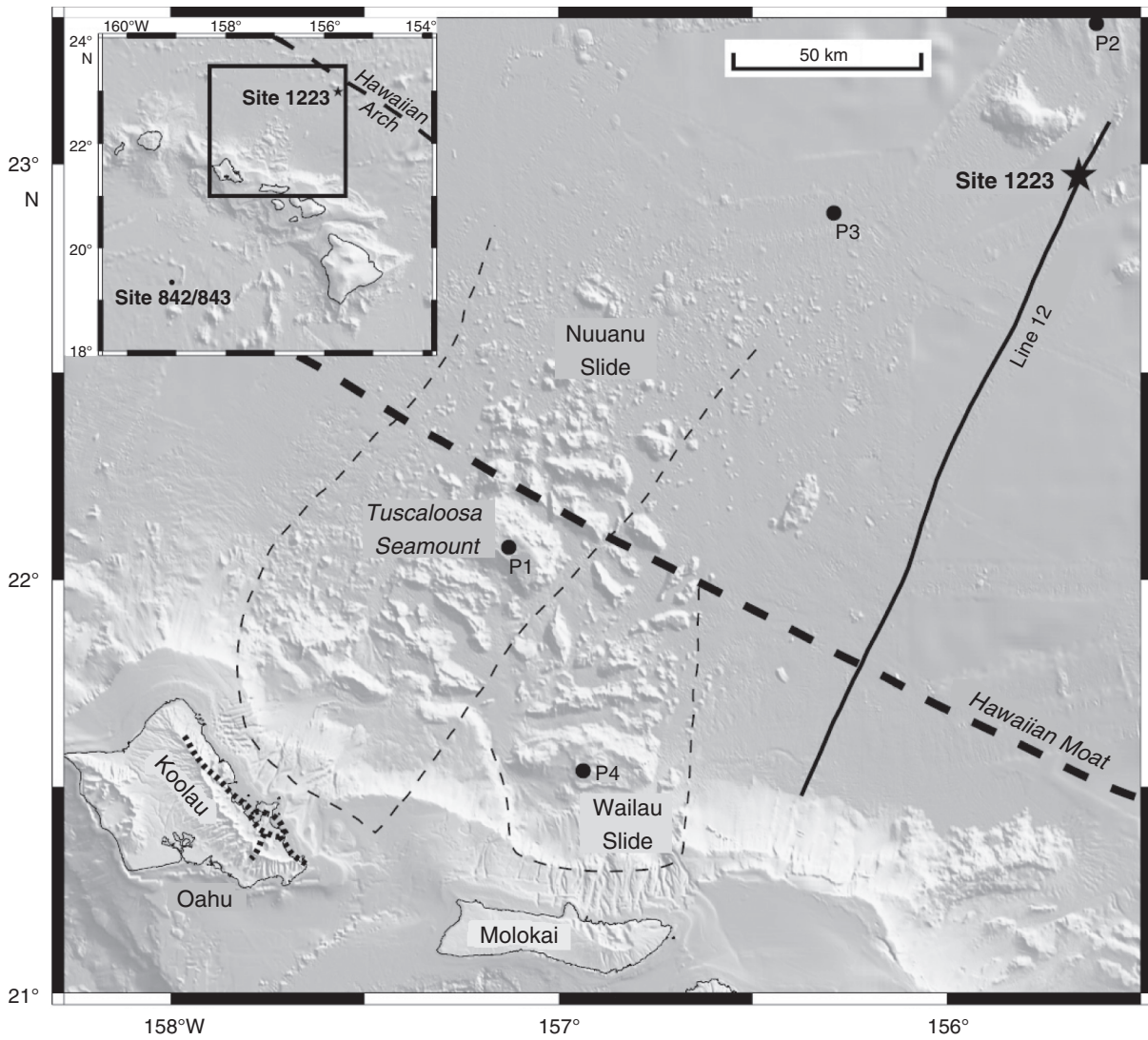
Figure F3. Seismic reflection record along Line 12 (Rees et al., 1993) shown in Figure F2, p. 19 (Garcia et al., 2006).
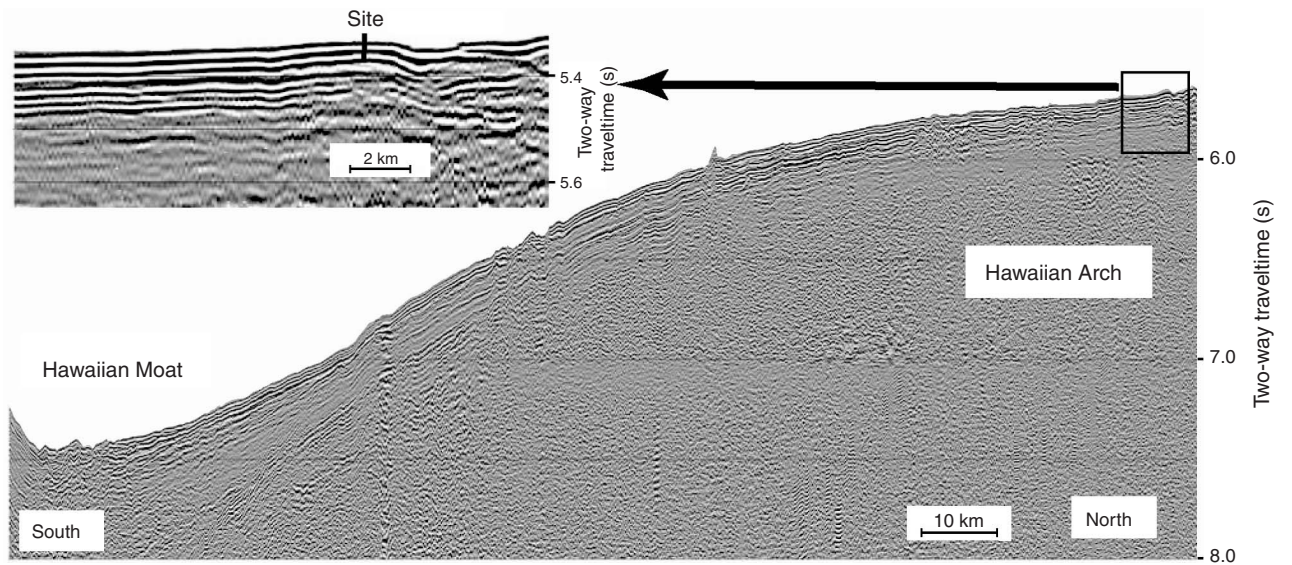
Figure F4. A. Vertical component spectrograms from day 350 in 2001 to day 27 in 2002 obtained by the shallow buried Guralp CMG 3 broadband seismometer (**Stephen et al.,** this volume). See color version of this figure on the CD-ROM or Web. (Continued on next page.)
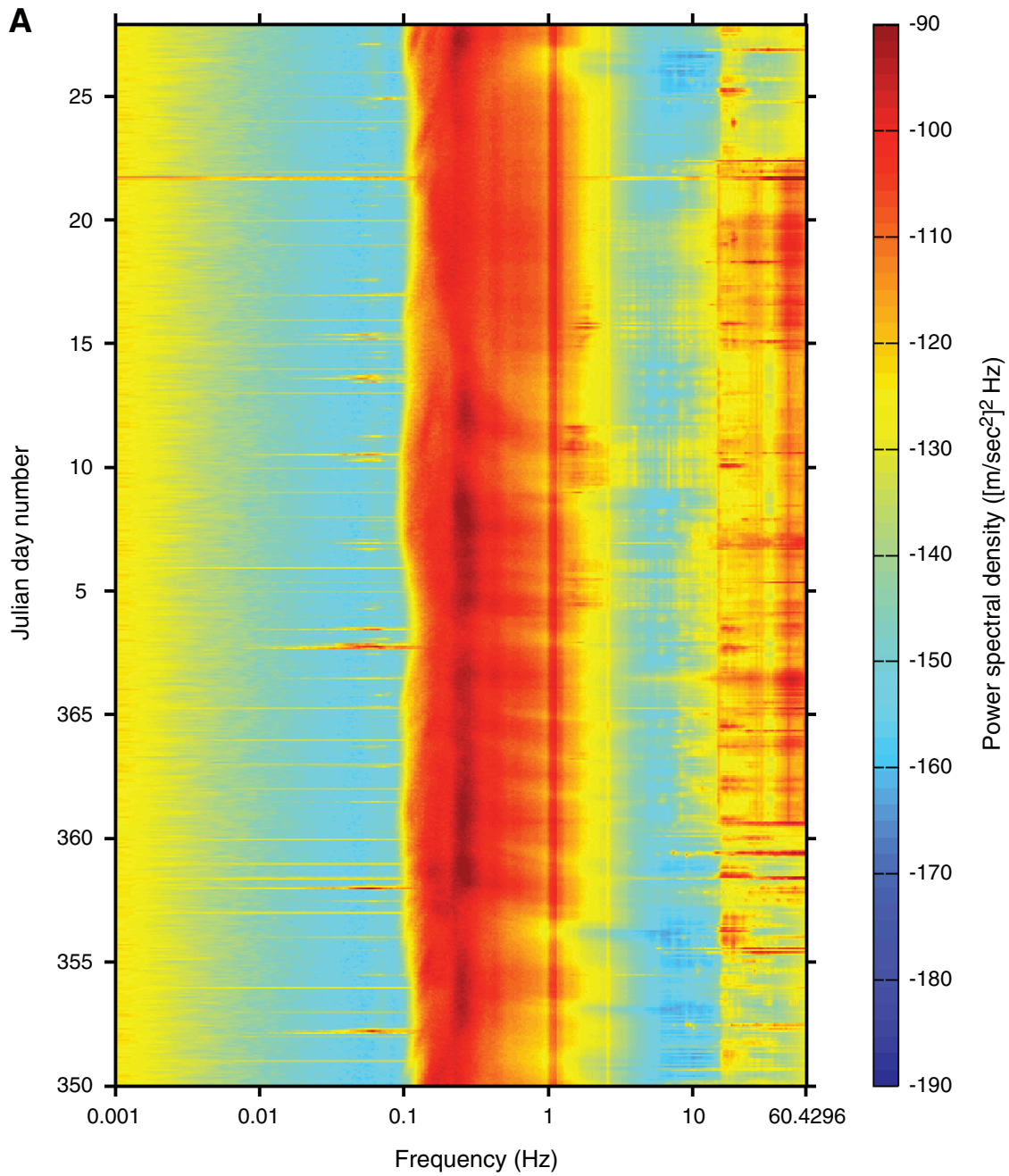
Figure F4 (continued). B. Horizontal component (1) Spectrograms from day 350 in 2001 to day 27 in 2002 obtained by the shallow buried Guralp CMG 3 broadband seismometer (**Stephen et al.,** this volume). The frequency band between 0.1 and 2 Hz is very noisy, typical of the double-frequency microseism and holu spectra. The horizontal component shows much higher noise below 0.01 Hz than the vertical component.
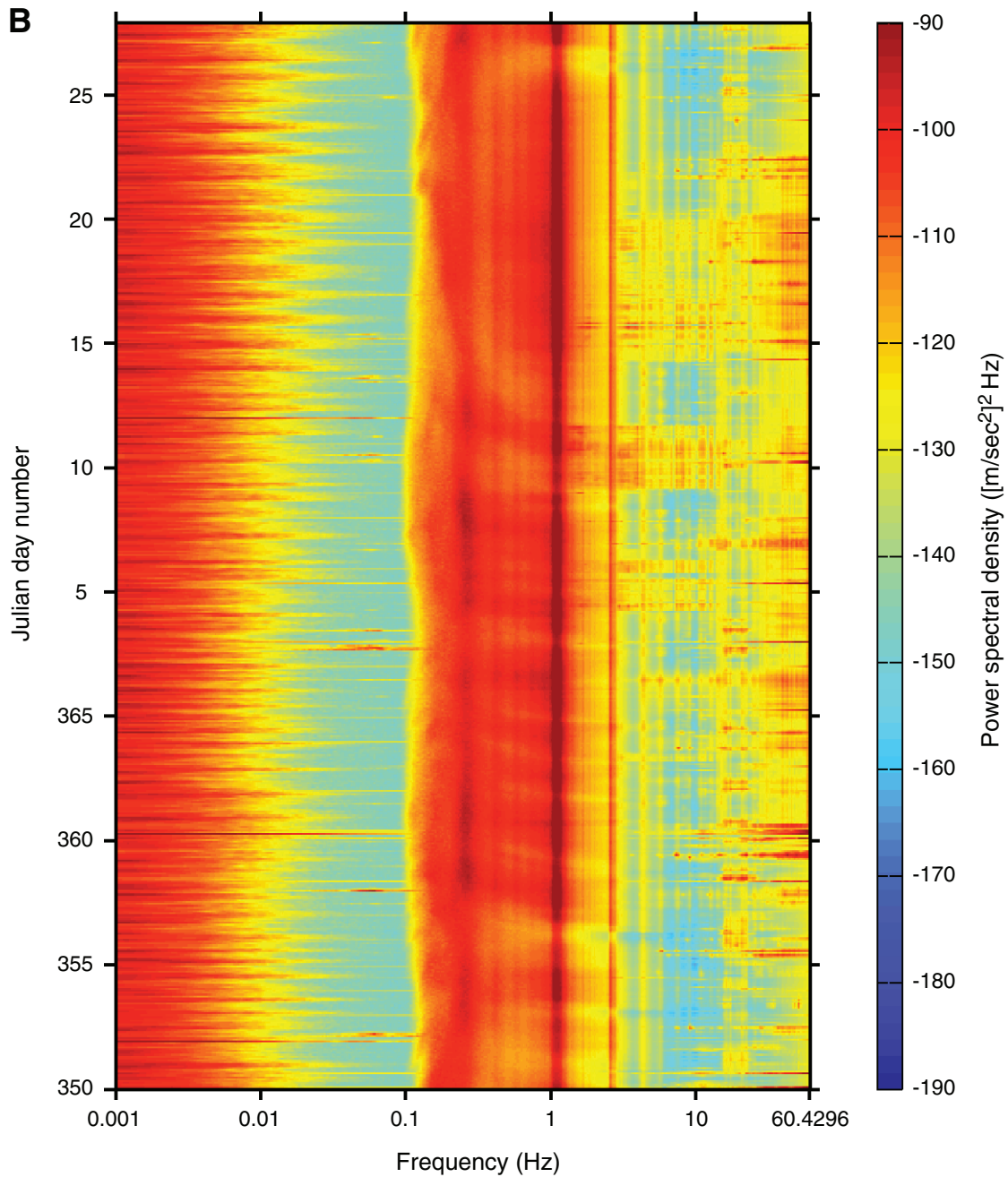
Figure F5. Noise spectra obtained by the H2O broadband seismometers (CMG-3) (H**) and the short-period seismometers (E**) for (**A**) vertical and (**B**) horizontal channels. (**Stephen et al.,** this volume).
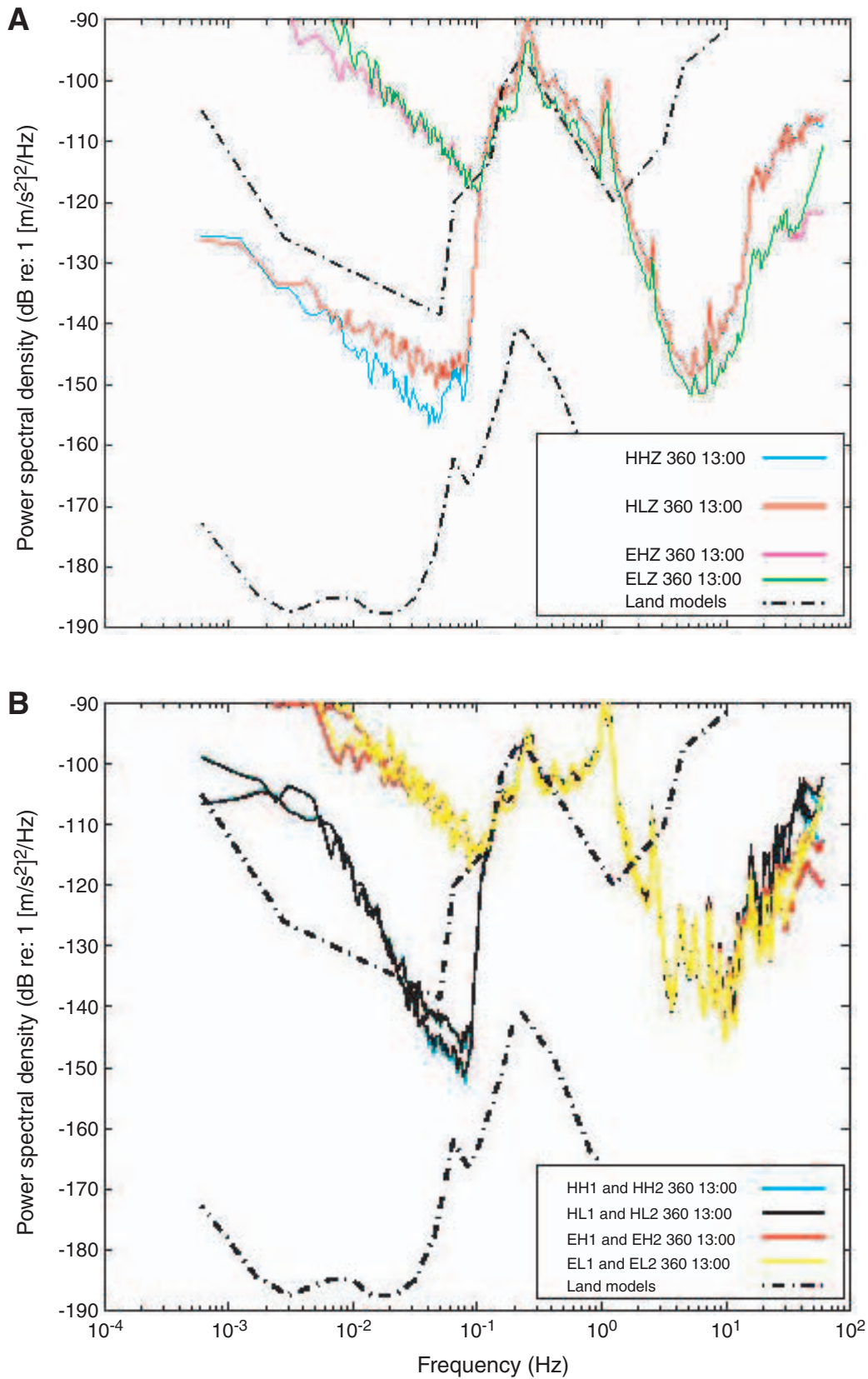
Figure F6. 3.5-kHz precision depth recorder (PDR) seismic record. Two distinct reflectors are seen at 13 and 38 ms. The deeper reflector corresponds to the basalt basement. The shallow one is not as clear, but it may be a layer of porous radiolarians.
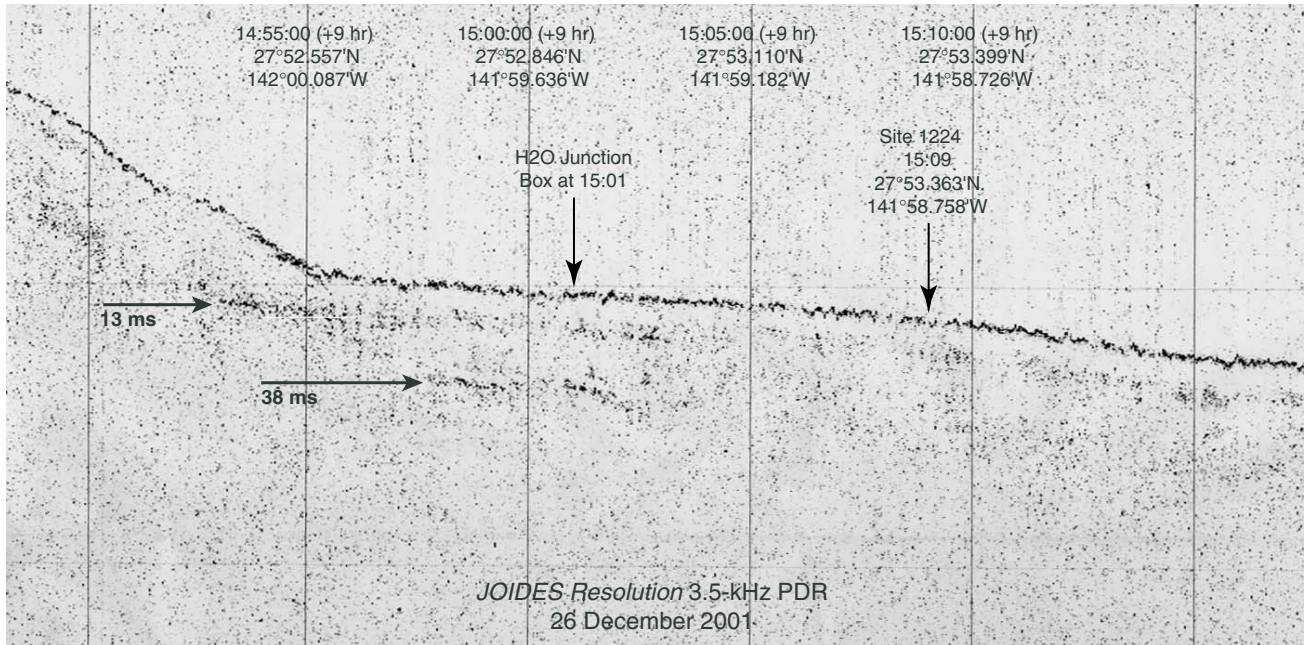
Figure F7. Core description of Site 1224 (H2O site) (Stephen, Kasahara, Acton, et al., 2003).
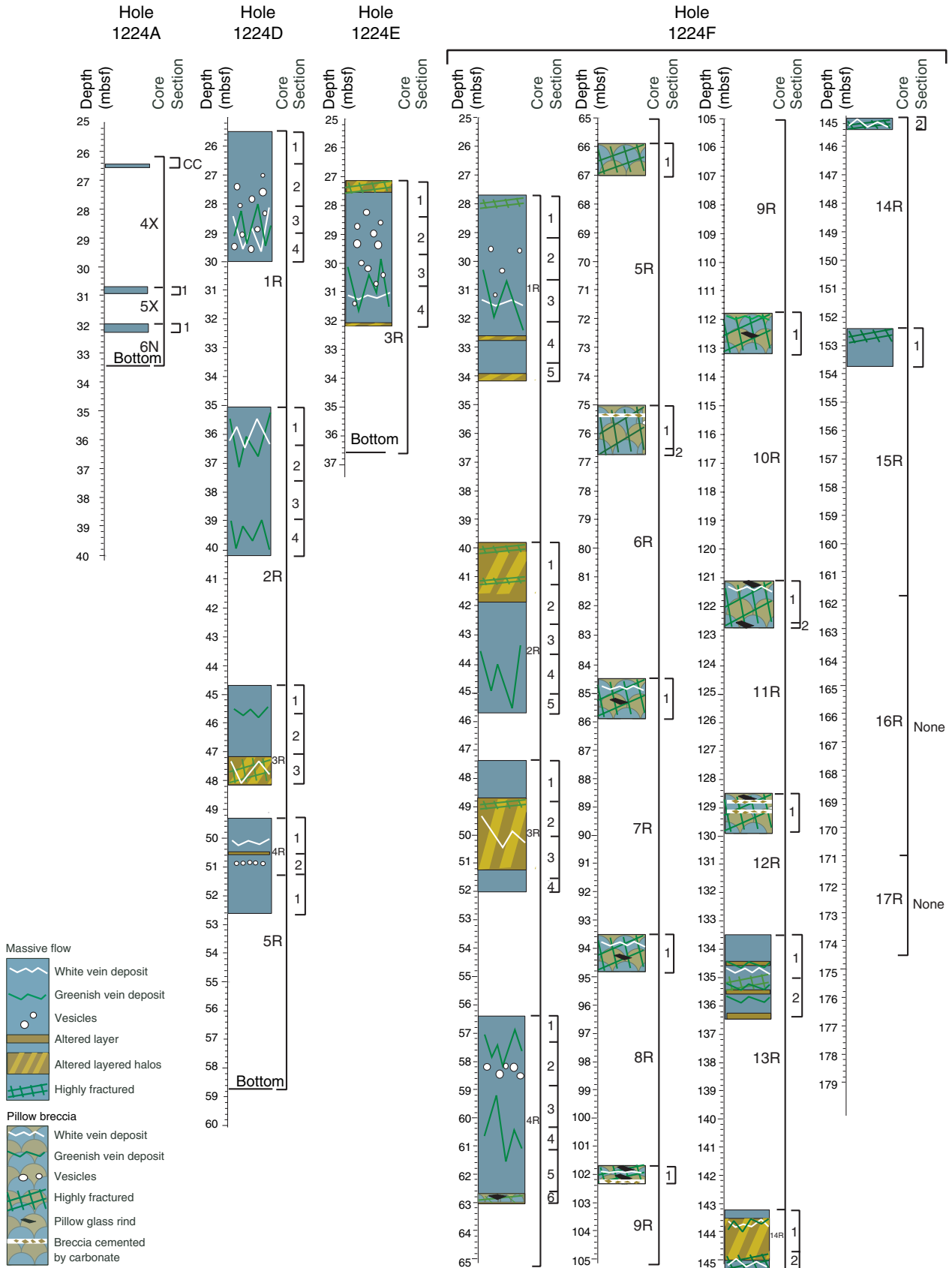
Figure F8. A. Distribution of major chemical elements (**Haraguchi and Ishii,** this volume). Note that TiO_2 contents and FeO show characteristics of ferrobasalt. In particular, the TiO_2 is extremely high below 130 mbsf. (Continued on next two pages.)
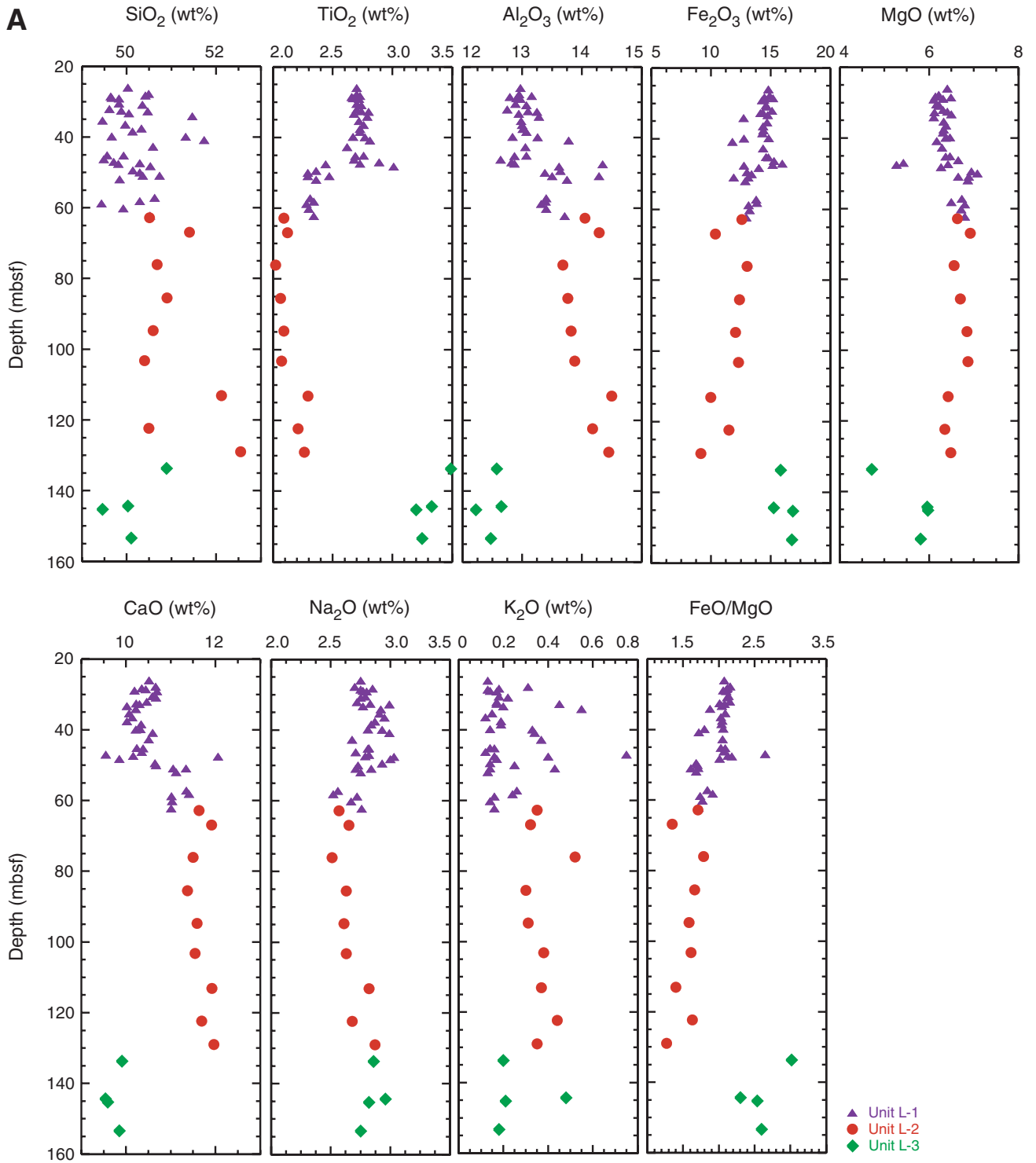
Figure F8 (continued). B. TiO$_2$ with depth (**Lustrino,** this volume). (Continued on next page.)
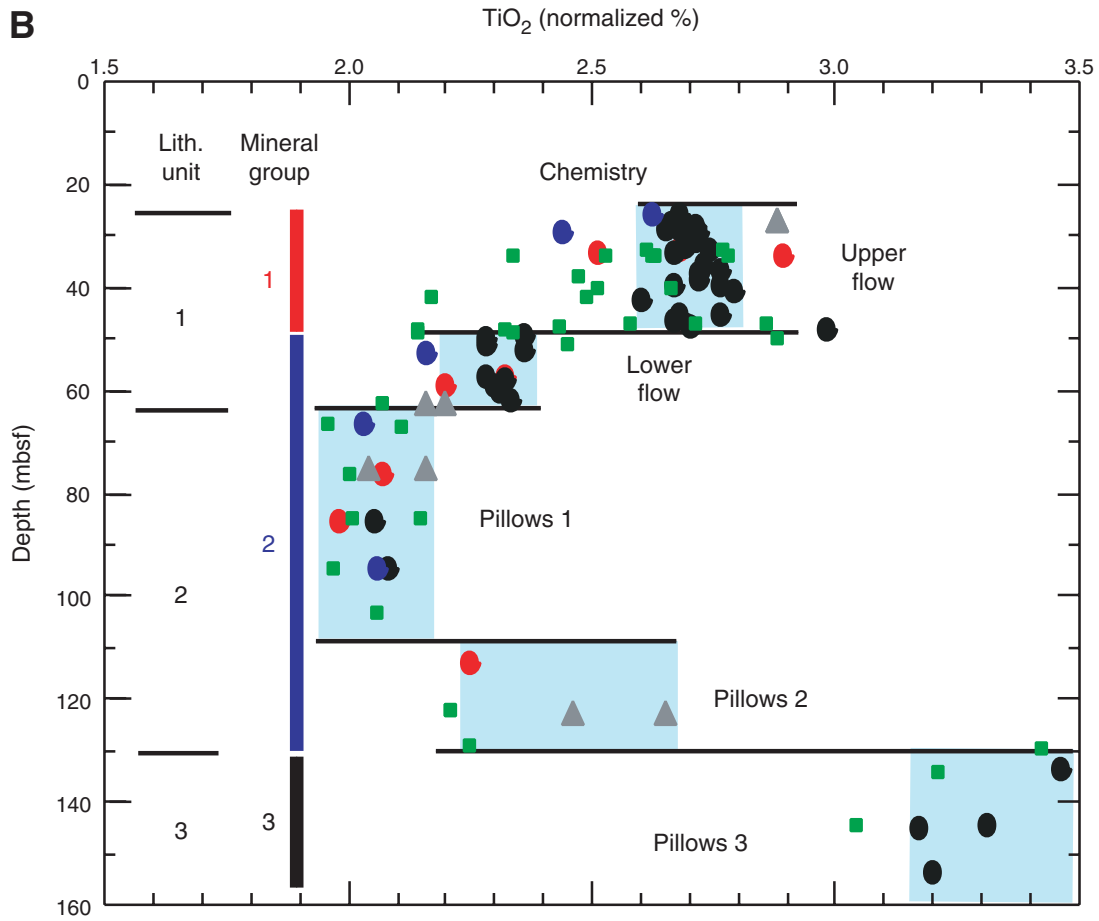
Figure F8 (continued). C. Nb, Zr, Y, and Cr variations with depth (**Lustrino,** this volume).
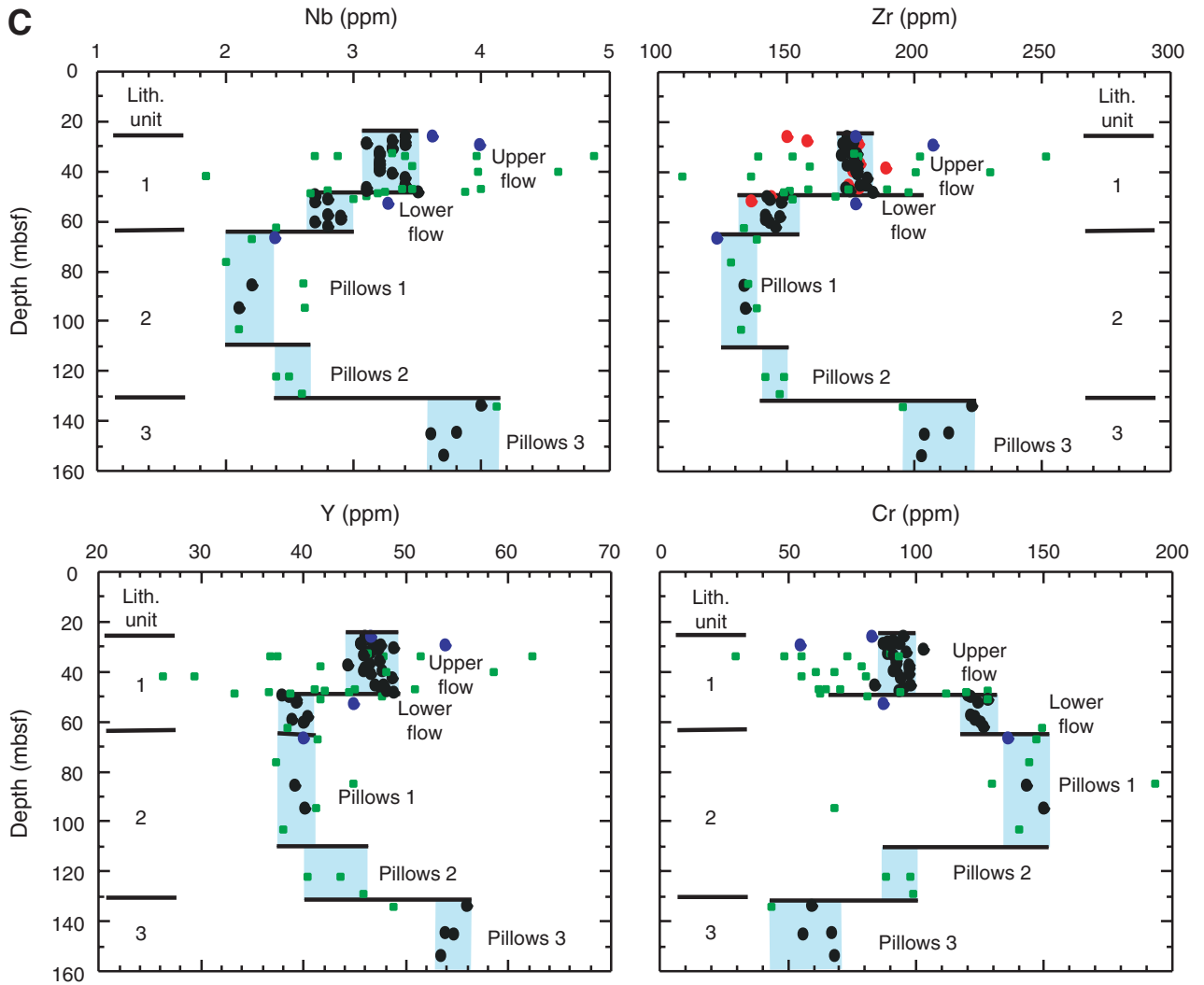
Figure F9. Relation of Y and Zr for Hole 1224F core samples (Haraguchi and Ishii, this volume). The Y/Zr ratio in Hole 1224F is an the extension of normal mid-ocean-ridge basalt (N-MORB) and enriched MORB (E-MORB), but quite different from ocean island basalt (OIB).
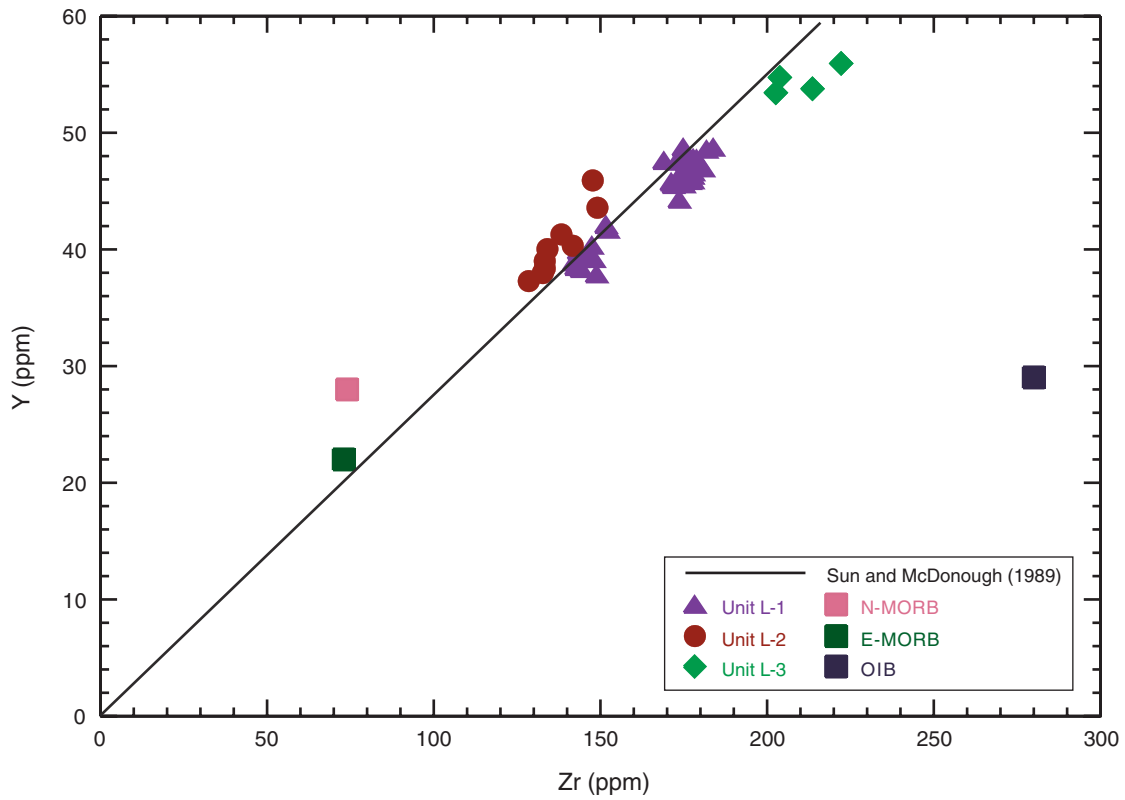
Figure F10. Temperature, density, porosity, *P*-wave velocity, and *S*-wave velocity in Hole 1224F (**Sun et al.,** this volume).
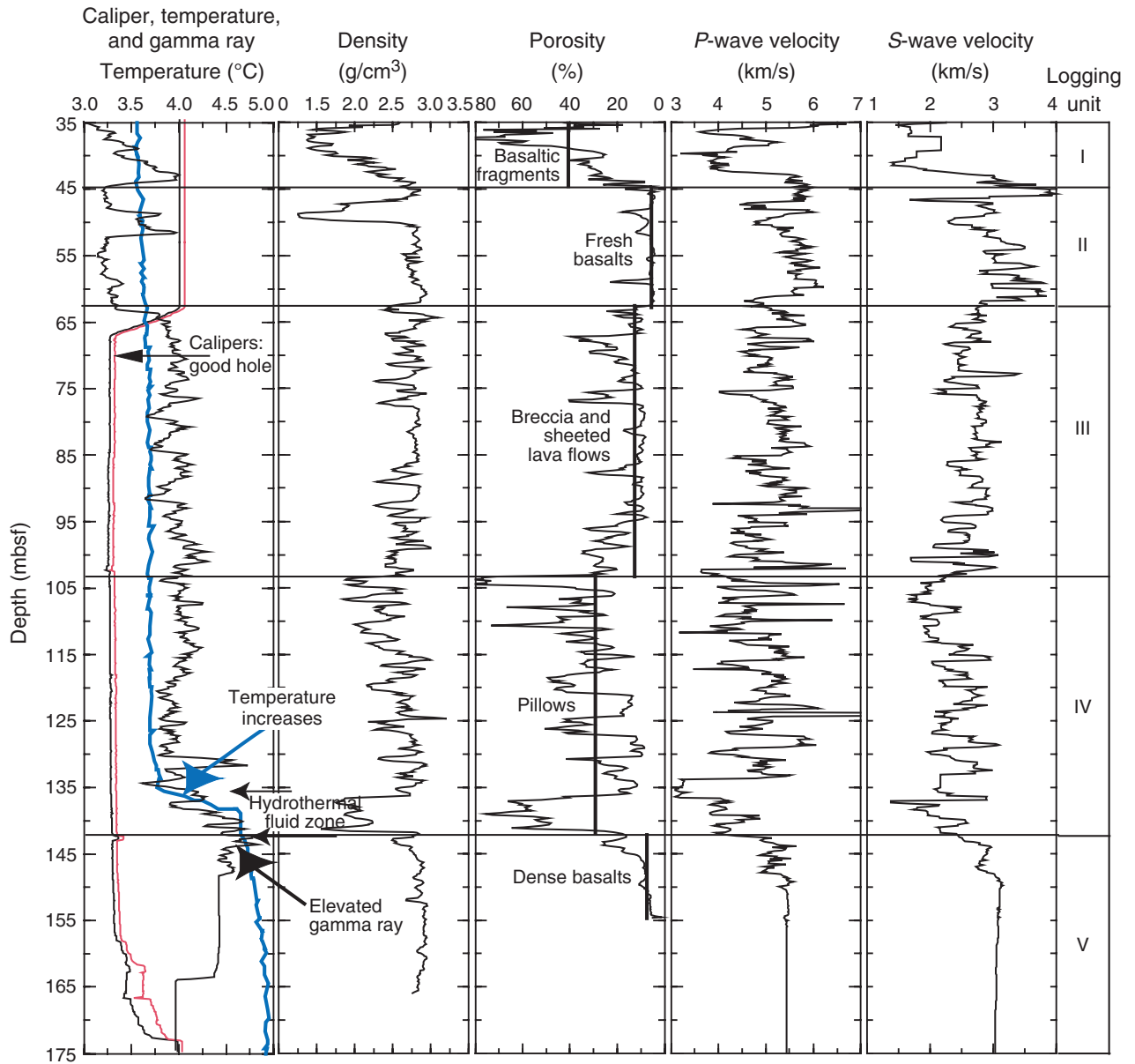
Figure F11. Logging results and synthesis units (S1–S7) in Hole 1224F. Arrows indicate unit boundaries.
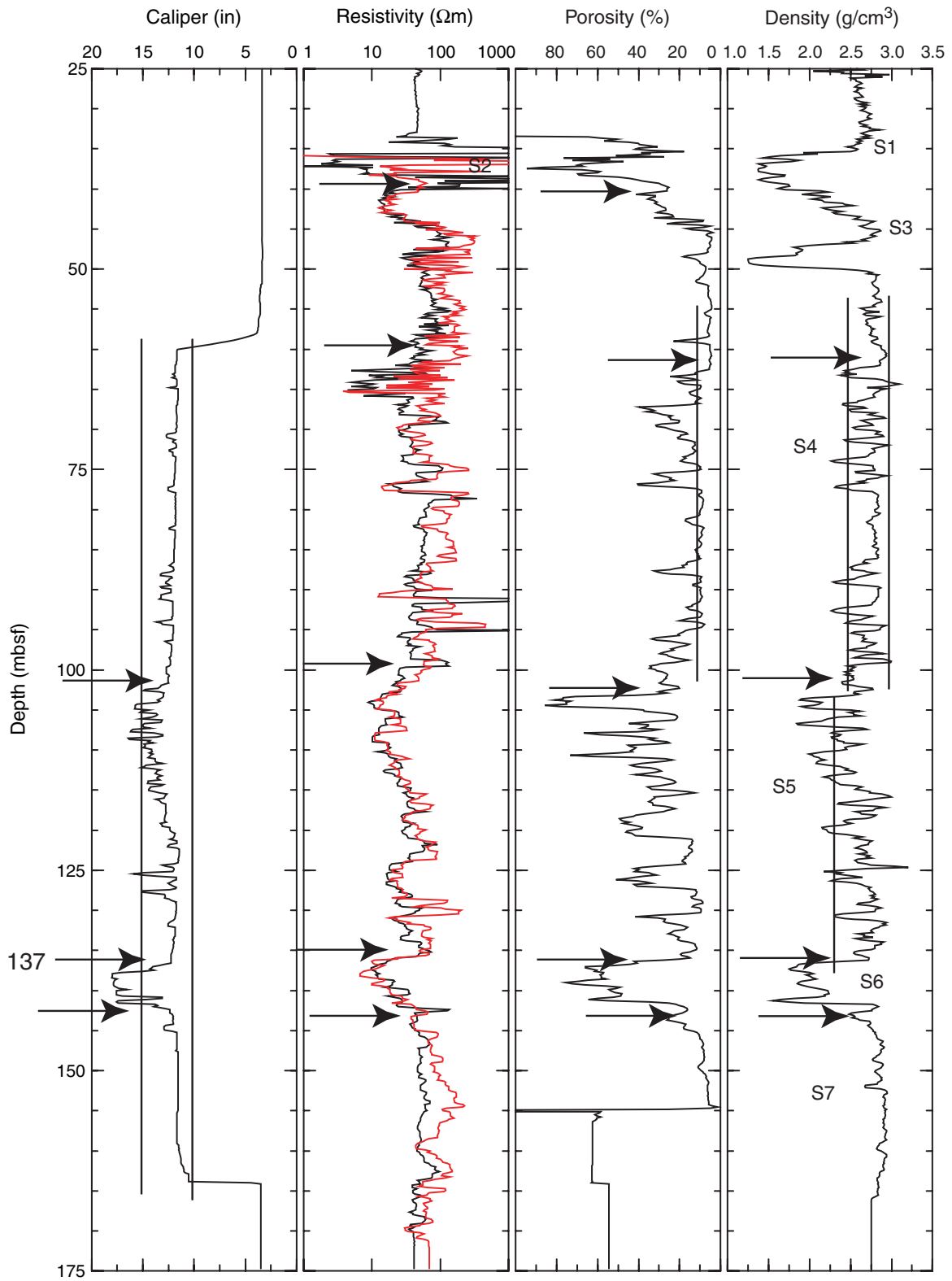
Figure F12. *P*-wave velocities and synthesis units (S1–S7) in Hole-1224F. Synthesis units are proposed by shipboard physical property measurements.
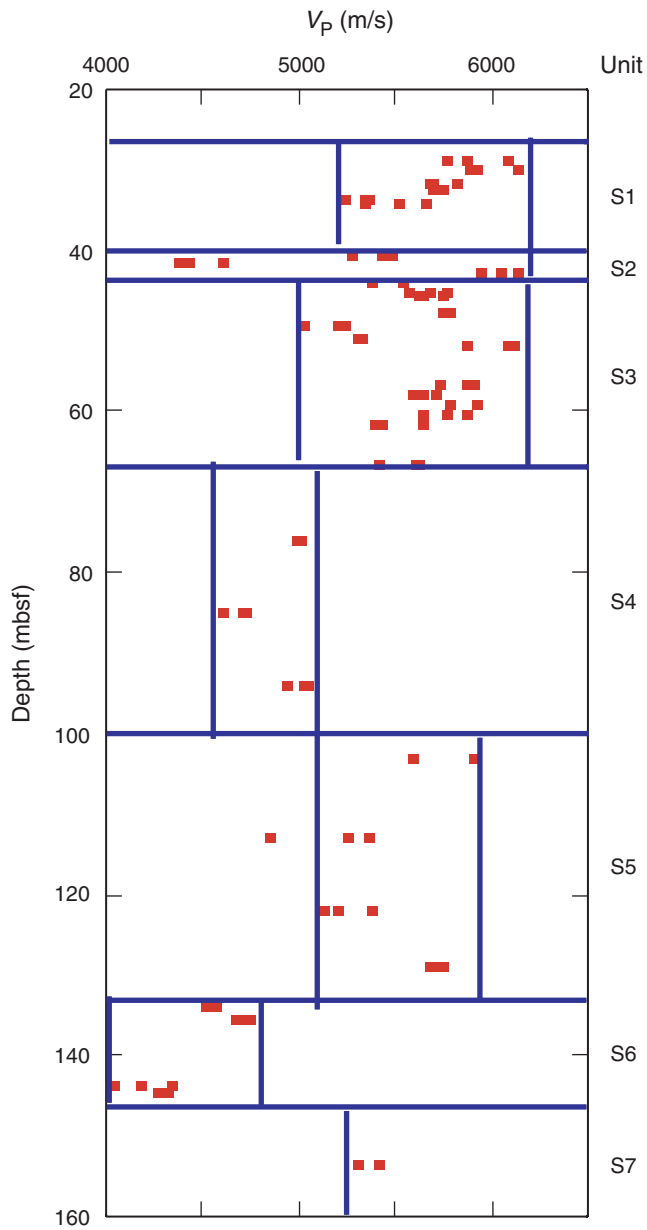
Figure F13. Comparison of logging and shipboard physical property measurement data on porosity, density, V_P, and V_S (**Sun et al.,** this volume). Laboratory measurements lie on the highest trends.
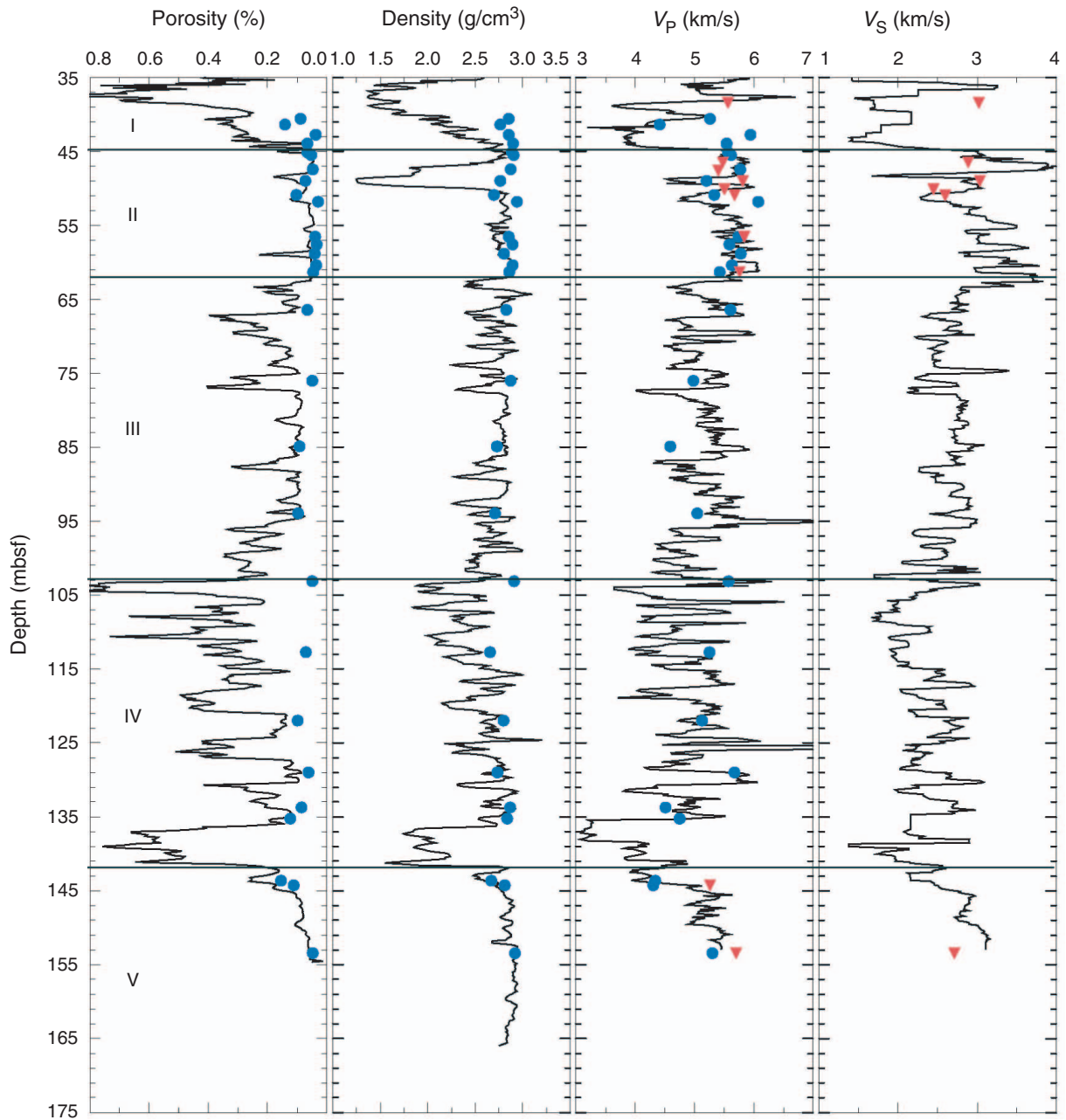
Figure F14. V_P and V_S measurements under pressure up to 100 MPa (**Sun et al.,** this volume). The results do not show drastic changes of velocity under pressure. This suggests that most of the velocity variations measured by logging are caused by cavities and larger fractures (on the order of a few centimeters).
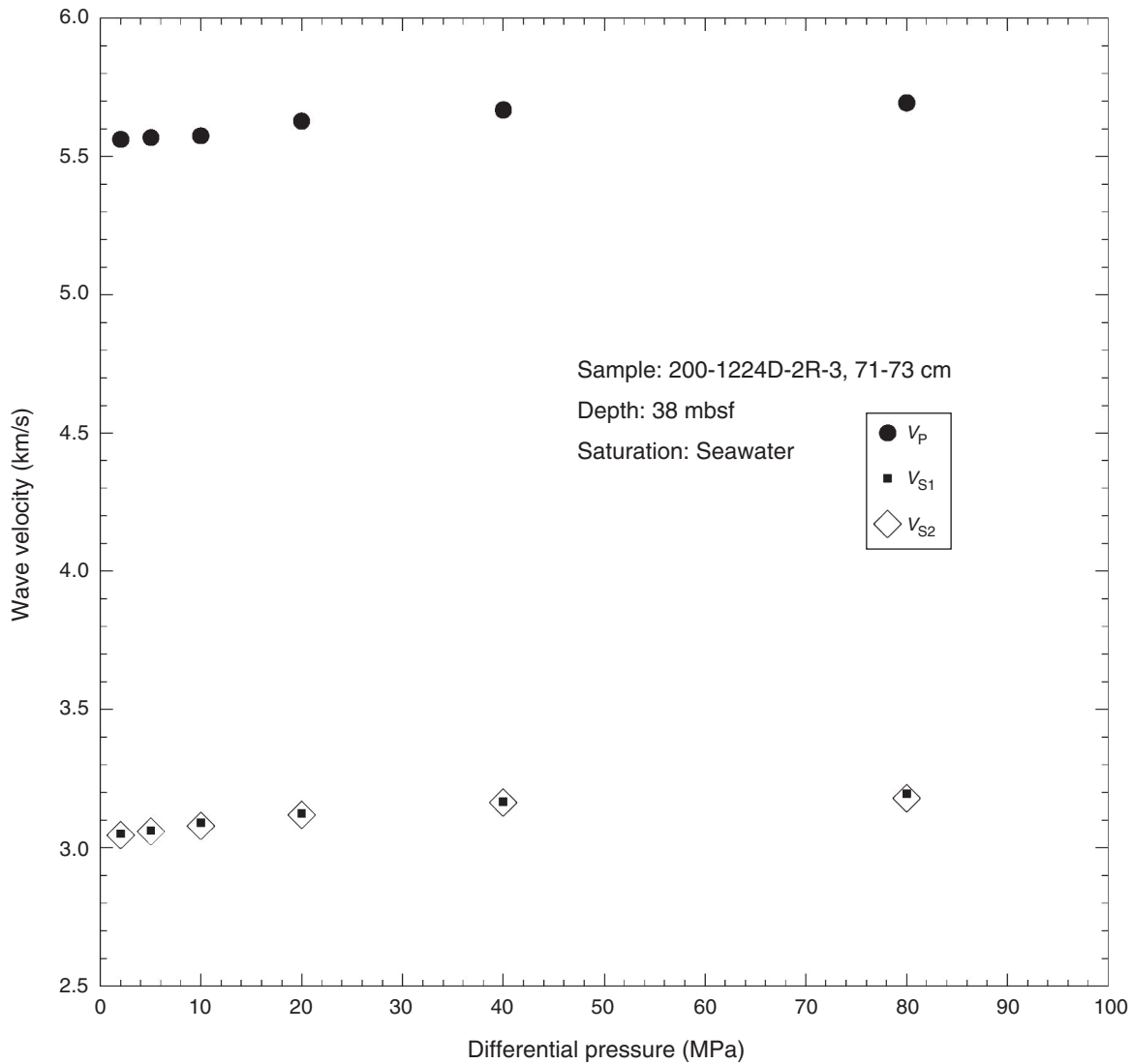
Figure F15. V_P estimated by using the Hole 1224F shipboard physical property measurements (Stephen, Kasahara, Acton, et al., 2003).
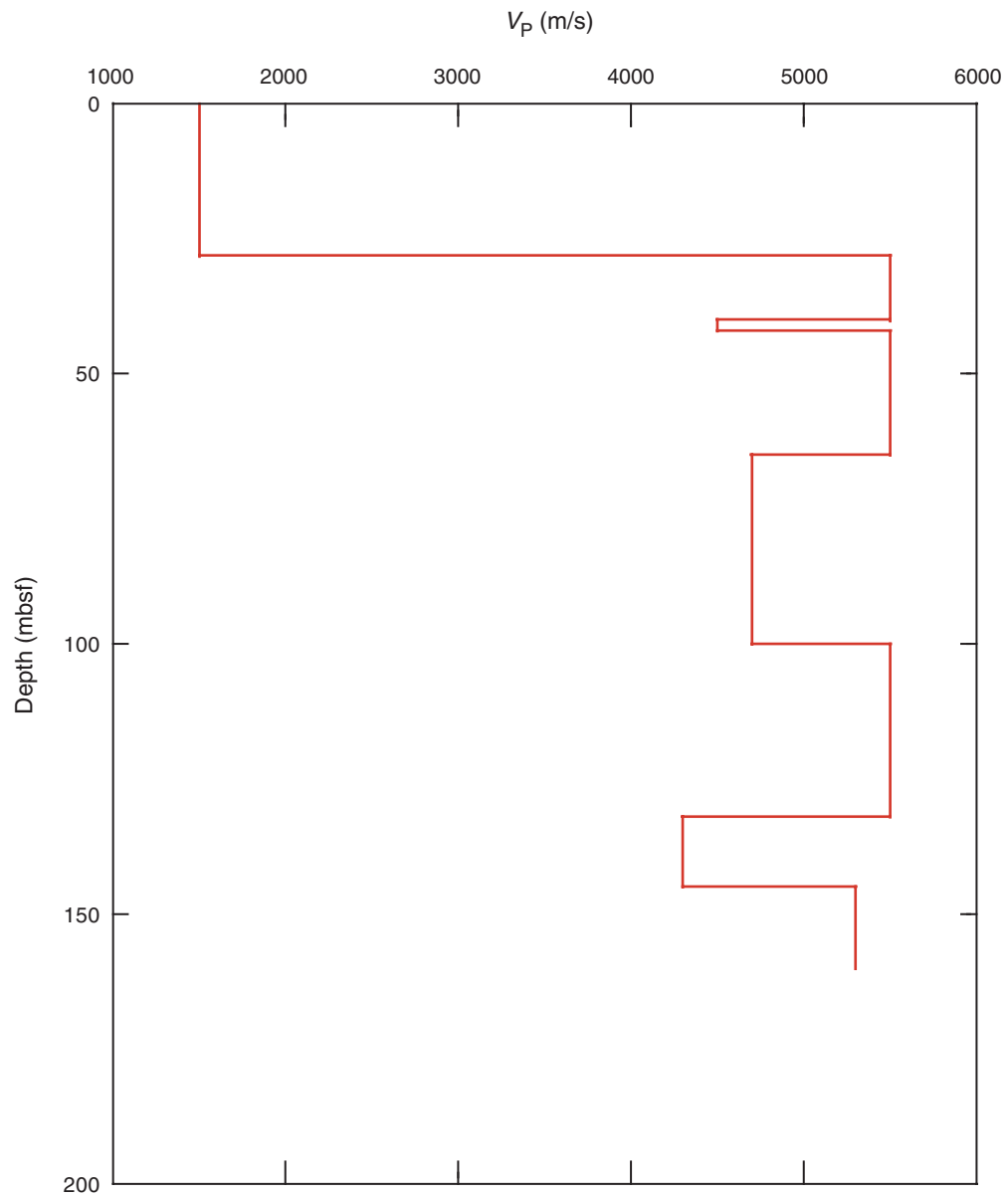
Figure F16. Synthetic reflection seismogram using logging V_P and density data (Sun et al., this volume). RC = reflection coefficient, BP = bulk porosity.
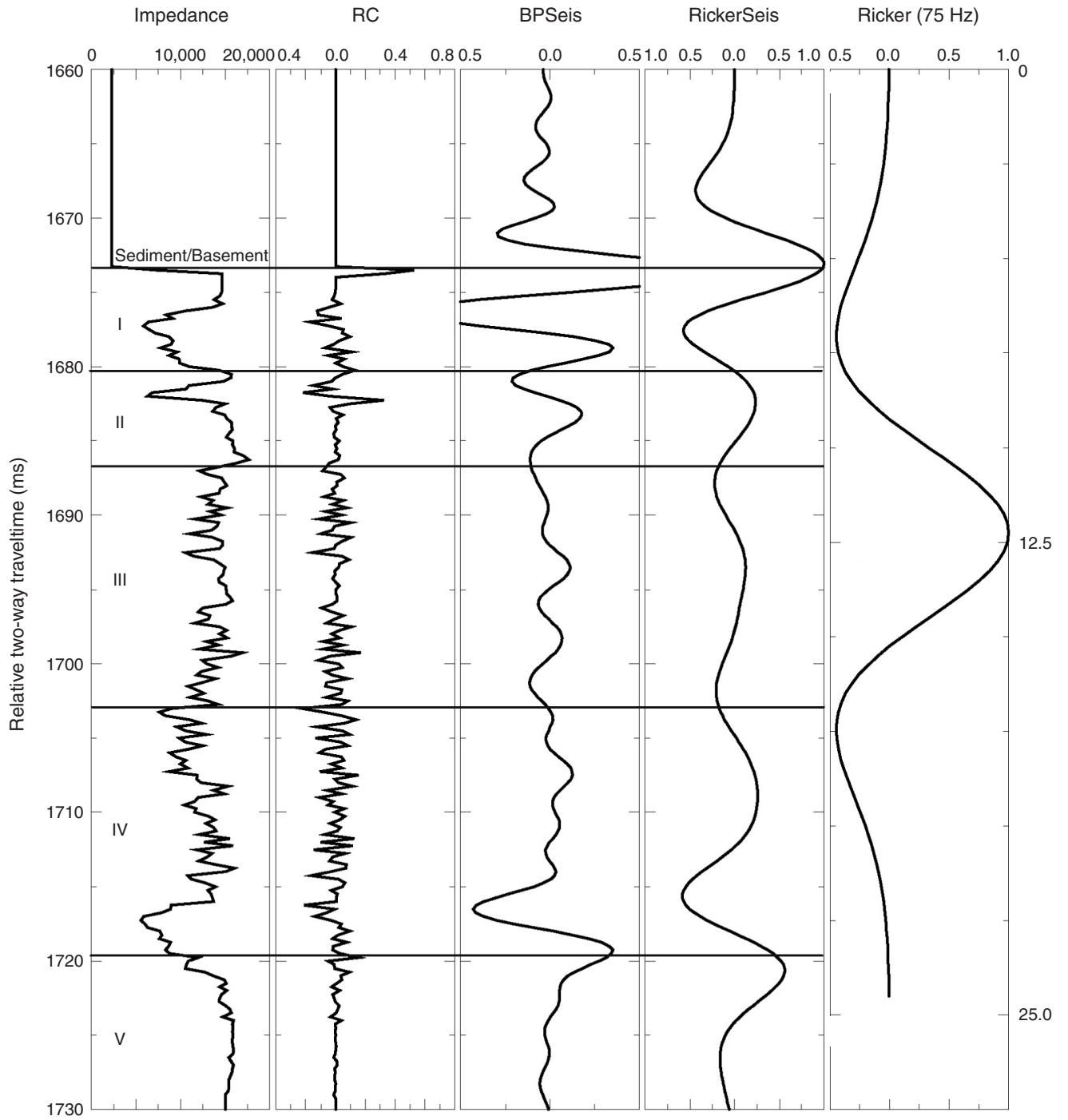
Figure F17. Comparison of observed seismic reflection records with synthetic seismograms using a 75-Hz Ricker wavelet (Sun et al., this volume). SCS = single-channel seismic.
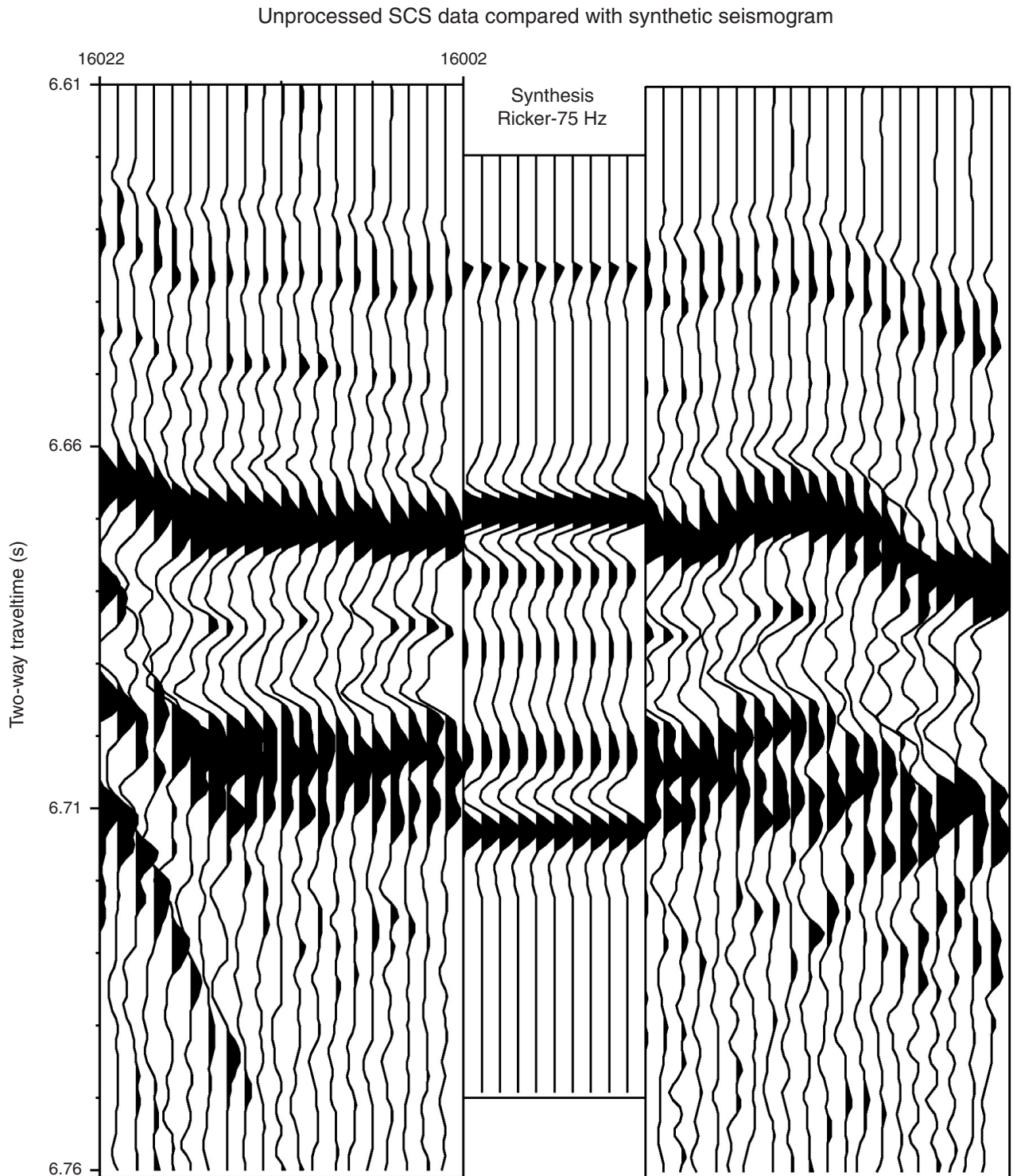

Unprocessed SCS data compared with synthetic seismogram

Figure F18. Seismic reflection record and its interpretation using synthetic seismograms obtained from logging data (**Sun et al.,** this volume). Logging Unit LG-V is the deepest horizon identified on the seismic refection record. This suggests that below logging Unit LG-V major fractures and/or hydrothermal circulation may not exist. SCS = single-channel seismic.
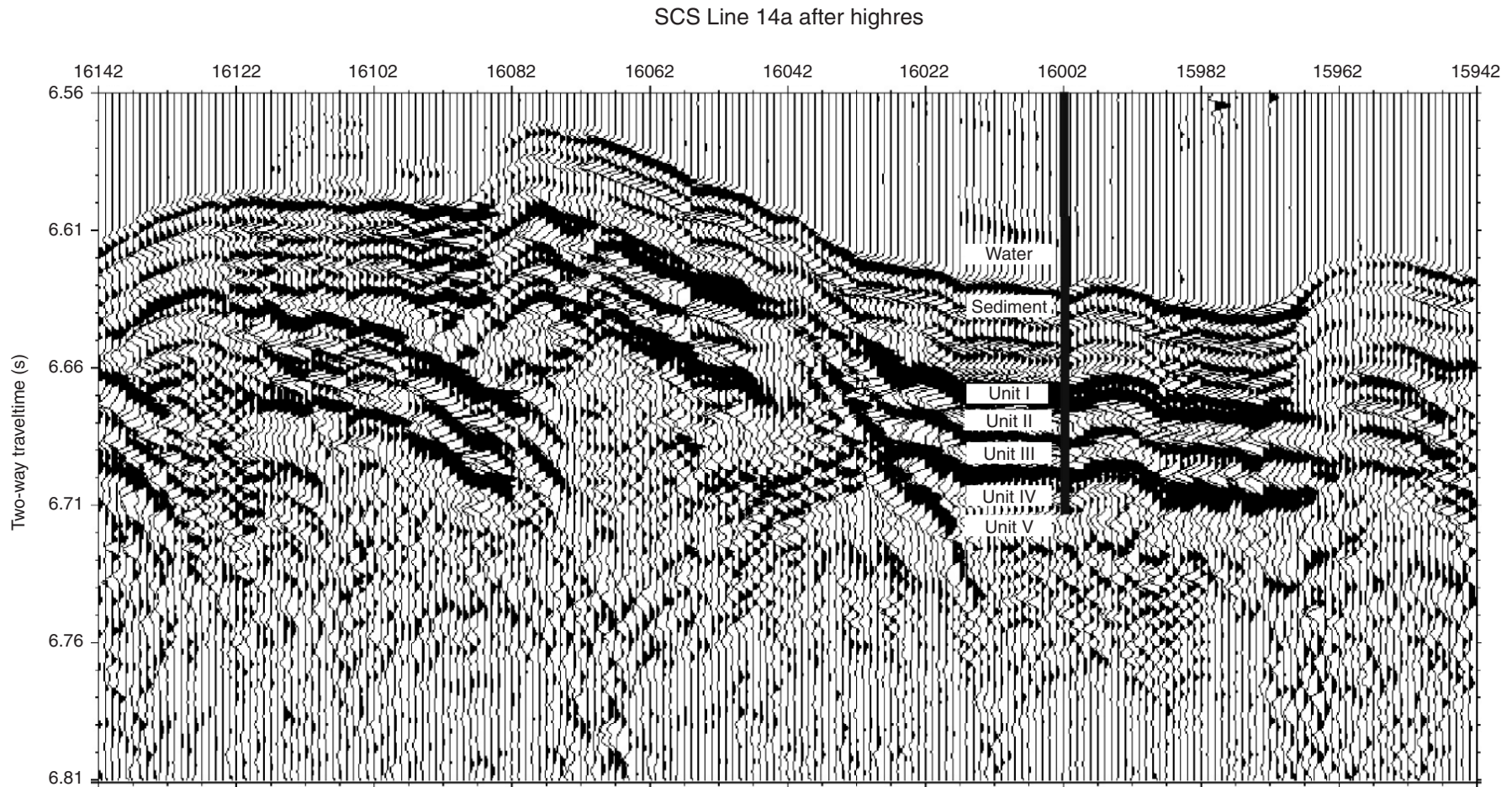

SCS Line 14a after highres

Figure F19. Photomicrographs of filamentous fungal structures within CaCO$_3$-filled vesicles in basalt at 51 mbsf in lithologic Unit L-2 (Schumann et al., 2004). Scale bars = (A) 1.5 mm, (B) 10 µm, (C, D) 20 µm. Hyphae divided by septa are shown by arrows in (C).
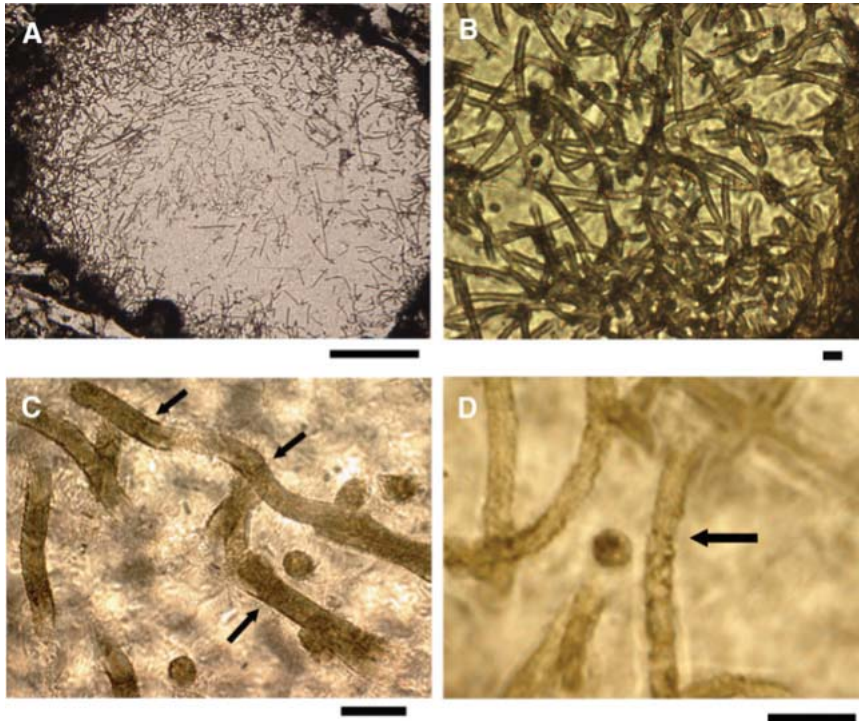
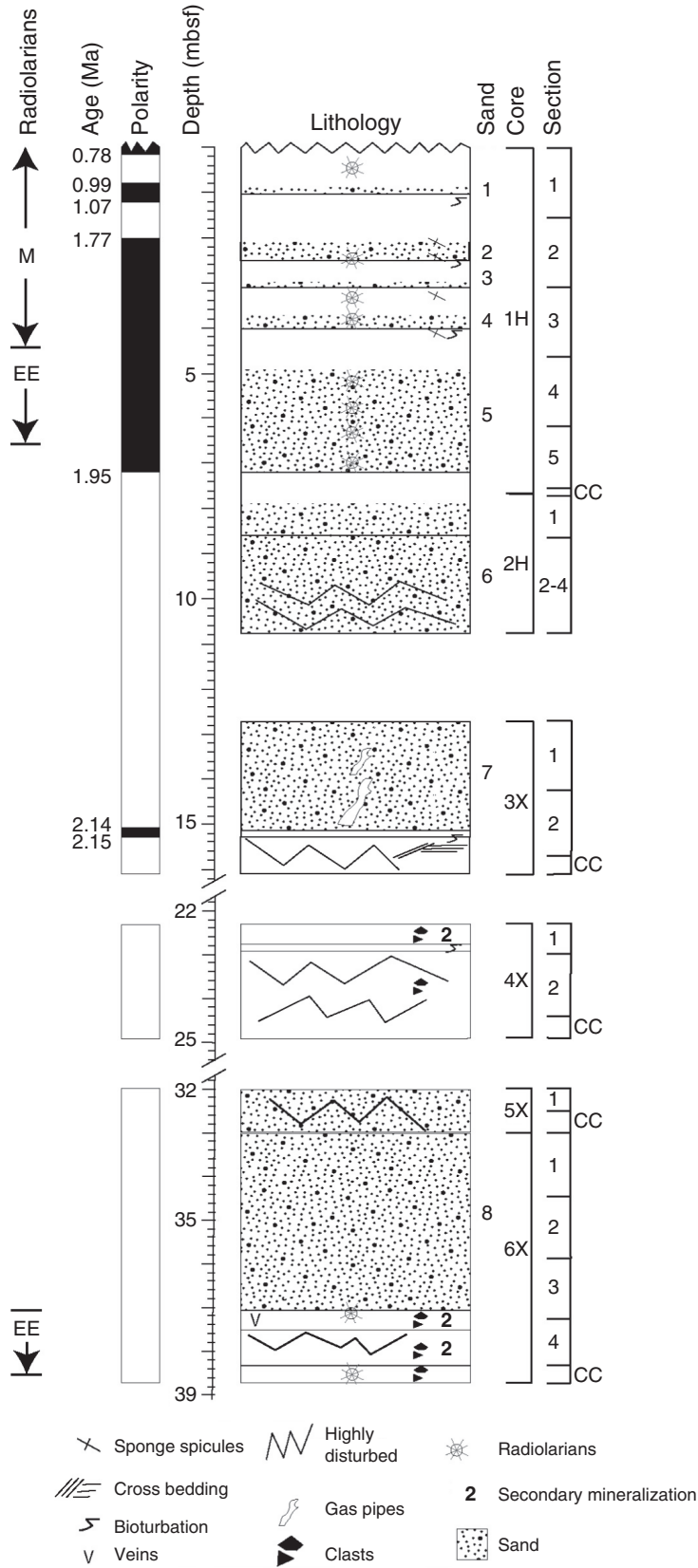**Figure F20.** Lithologic units of Hole 1223A (Garcia et al., 2006). M = Eocene and younger, EE = early Eocene.

Figure F21. Bulk density of Site 1223 (Stephen, Kasahara, Acton, et al., 2003). GRA = gamma ray attenuation.
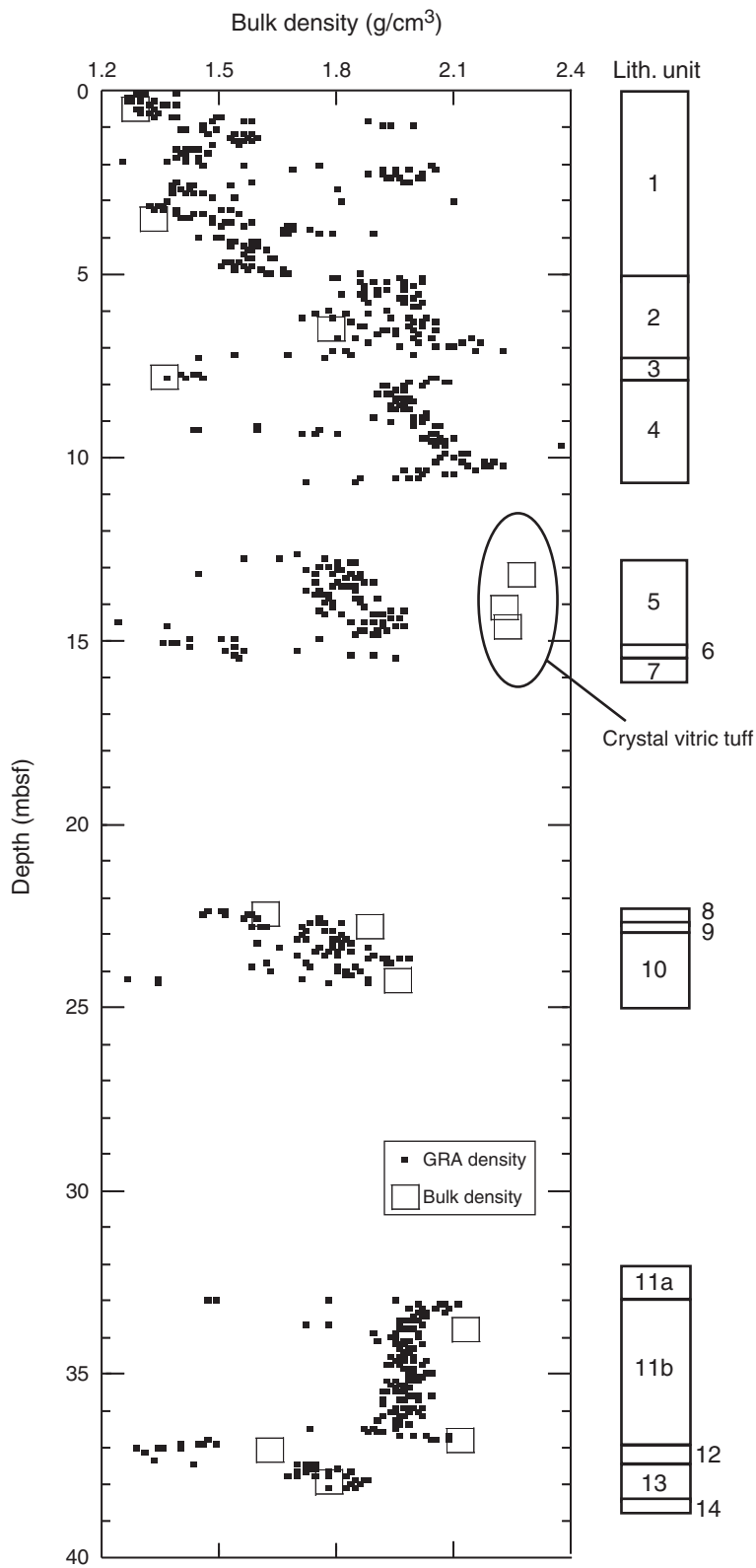
Figure F22. Velocities at Site 1223 (Stephen, Kasahara, Acton, et al., 2003). PWL = *P*-wave logger, PWS = *S*-wave sensor.
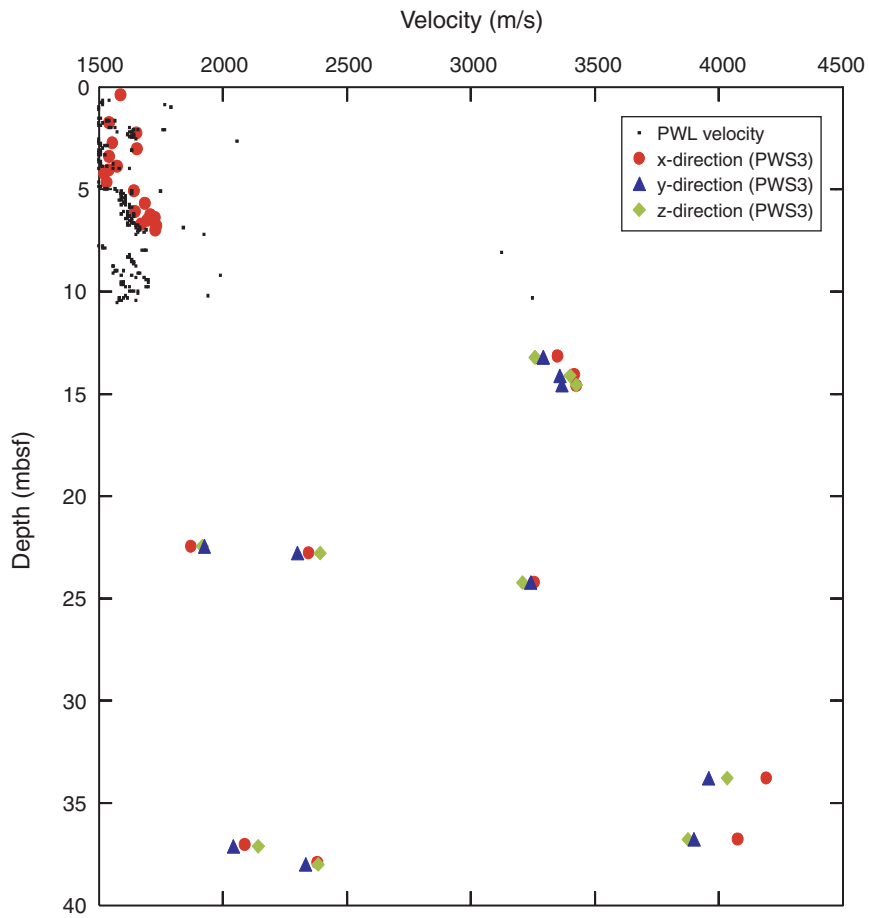
Figure F23. MgO versus SiO_2 and CaO for glass sands from Layers 1–8 of Hole 1223A. The range of values for sands from the Koolau and East Molokai group are also shown. (Reprinted from Garcia et al., 2006, with permission from Elsevier.)
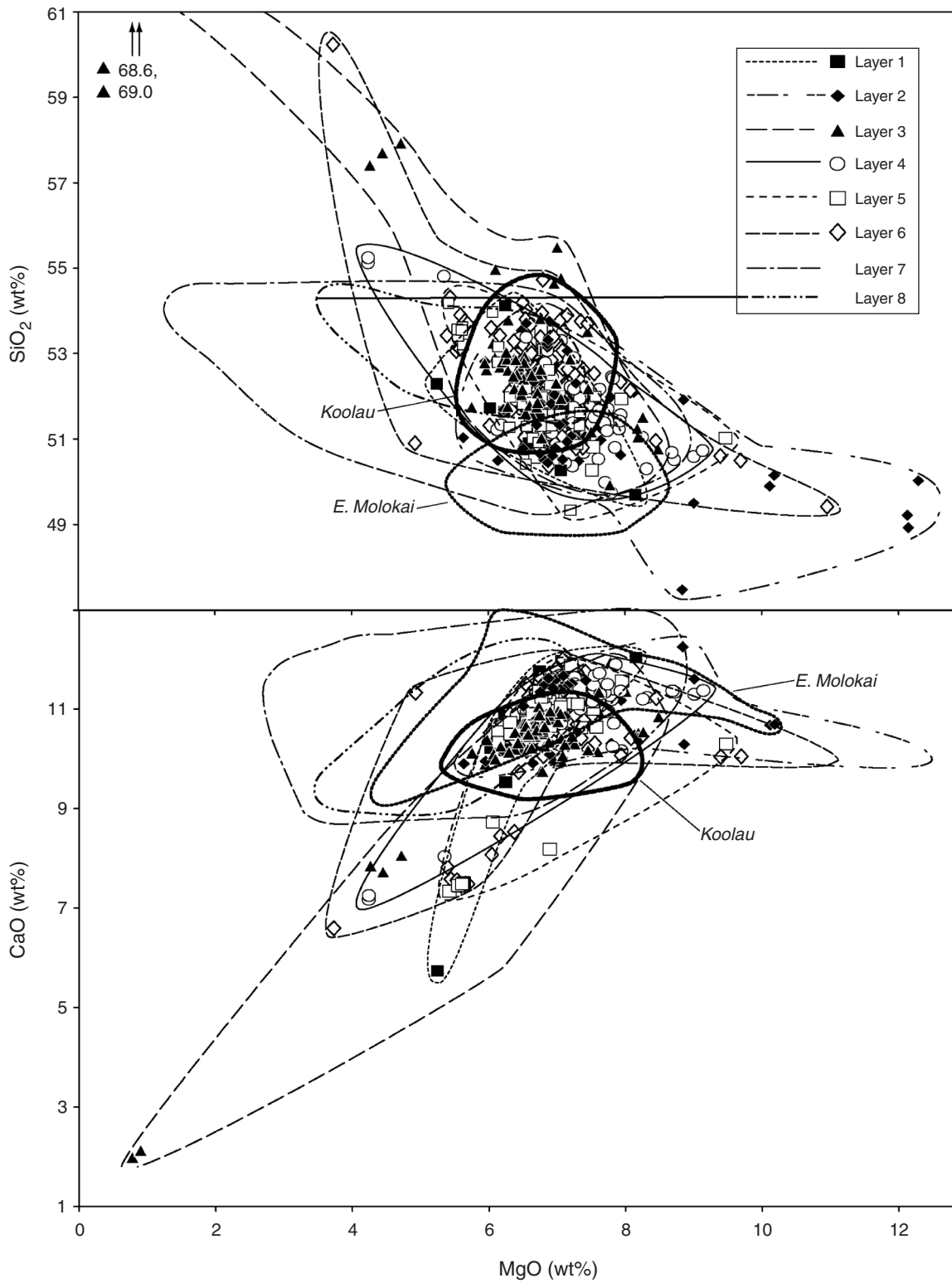
Table T1. Site 1224 summary of lithology, geochemistry, logging, and physical properties.

Synthesis unit	Depth (curated mbsf)	V_p (km/s)	Logging unit (mbsf)	Lithologic unit (curated mbsf)	Chemistry				General description
					TiO$_2$ (wt%)	Nb (ppm)	Zr (ppm)	Y (ppm)	
S-0A	0–14	1.5?		Sedimentary layer					Yellow to brown clay+radiorarian
S-0B	14–28			Sedimentary layer					Brown-red clay
S-1	28–38	5.5–6.0	LG-I (28–45)	Unit L-1 (28–62.7)	2.5–2.8	3.1–3.3	150–160	44–48	Upper flow of Unit L-1
S-2	38–41	4.2–5.5							
S-3	41–65	5.0–6.0	LG-II (45–63)		2.1–2.4	2.9–3.0	130–160	38–42	Lower flow of Unit L-1
S-4	65–100	4.5–5.0	LG-III (53–103)	Unit L-2 (62.7–133.5)	1.9–2.1	2.0–2.2	~130	38–42	Pillow 1 of Unit L-2
S-5	100–137	4.7–6.0	LG-IV (103–142)		2.2–2.6	2.2–2.3	~145	40–46	Pillow 2 of Unit L-2
S-6	137–143	4.0–4.7		Unit L-3 (133.5–161.7)					Pillow 3
S-7	143–174.3	5.3	LG-V (>142)		3.0–3.5	3.6–4.0	200–220	43–56	

Notes: Unit boundaries are different among measurements (see shaded blocks). S-0 to S-7 are based on physical properties. Logging units are based on wireline length. Chemistry data from **Lustrino,** this volume.